

2020 Geophysical Interpretation Report

(Regional Airborne Interpretation, DIGHEM Interpretation, IP/RES Interpretation)

on the
Indian River (IND) Property
Dawson City, Yukon

GRANT_NUM	LABEL	GRANT_NUM	LABEL
YC36103 - 112	Ind 1 - 10	YC95578 - 579	IND 105 - 106
YC44987 - 996	Ind 11 - 20	YC96177 - 200	IND 107 - 130
YC61018 - 039	IND 21 - 42	YC96163 - 168	IND 131 - 136
YC96113 - 124	IND 43 - 54	YF70101 - 104	IND E 1 - 4
YC96101 - 112	IND 55 - 66	YF70121 - 124	IND E 21 - 24
YC96137 - 162	IND 67 - 92	YF70135 - 138	IND E 35 - 38
YC96125 - 136	IND 93 - 104	YF70145 - 148	IND E 45 - 48

NTS: 1:50,000 115O13

UTM: 570000 E 7080000 N
NAD83 Zone 7

Dawson Mining District

Work Performed Between:
Geophysical Interpretation: March 1st – 15th, 2020

Prepared for White Gold Corporation
By GroundTruth Exploration

Written By: Matthew Hanewich
April 7th, 2020

Summary

The following report documents the geophysical interpretation completed on the Indian River (IND) property in March of 2020. The interpretation covers the entire IND property using historic aerial mag and radiometric data. It also uses data from the 2017 8.5km² aerial DIGHEM survey.

The property is wholly owned by White Gold Corp and is in the Dawson Mining district, centered roughly 25 km South of Dawson City.

Most of the conductive zones are associated with low resistivity (high conductivity) areas identified by 3D inversion modelling of DCIP data. Some high chargeability anomalies overlie high gold areas, mostly near the edges of low resistivity zones. The EM results define a pronounced E-W trending conductor mapped from EM in-phase and quadrature waveforms at different frequencies. These conductors are sub-parallel with the magnetic lineaments mapped from aeromagnetic data and correlate well with the general trend of the gold in soil geochemical anomalies.

Table of Contents

Introduction	1
Location and Access	1
Claims	1
History and Previous Work	3
Geology	4
Regional Geology	4
Property Geology	7
2020 Geophysical Interpretation	7
Methods and Procedures	7
Analysis	7
Results and Interpretation	8
References	9
Statement of Expenditures	10
Statement of Qualifications	11

List of Figures

Figure 1: IND Location Map	2
Figure 2: Regional Geology Map	5
Figure 3: Correlation Chart of Major Geological Events - YT, AK	6
Figure 4: Property Geology Map	7
Figure 5: Claims Map and DIGHEM area	8
Figure 6: Chargeability at 40m depth with overlying Au in soil	9

List of Tables

Table 1: Claims Summary	1
-------------------------------	---

List of Appendices

Appendix I: Geophysical Report, Geophysical data

Introduction

The following report documents the geophysical interpretation completed on the Indian River (IND) property in March of 2020. The property is wholly owned by White Gold Corp and is in the Dawson Mining district, centered roughly 25 km South of Dawson City.

Results and interpretation are provided in the Geophysical report given in Appendix I.

Location and Access

The IND Gold Property is in the central-western part of Yukon, approximately 25km south of Dawson (Figure 1) near the confluence of the Yukon and Indian Rivers. The center of the property is located at UTM coordinates 570000 E, 7080000 N.

The property is in an unglaciated region of the Dawson Range. Elevations range from 440m to 1130m. Vegetation is typical of the Boreal forest, with mixed white and black spruce forests in valley bottoms, stunted black spruce and moss matt forests underlain by permafrost on north facing slopes and as elevation increases, transitioning into moss, talus and felsenmeer with increasing elevation. The typical climate of the area is moderate precipitation, warm summers, and cold winters. Access to the property is by all season road from Dawson.

Claims

The IND property is comprised of 188 contiguous claims in the Dawson Mining district (mapsheet 115O13, as of January 2020). There will be a total of 36 claims lapsing in April of 2020, which leaves 152 claims expiring in the spring of 2021 (Figure 5).

Table 1: Claims Summary

GRANT_NUM	LABEL	OWNER	DISTRICT	New Expiry	No. Claims
YC36103 - 112	Ind 1 - 10	White Gold Corp. - 100%	Dawson	3/15/2023	10
YC44987 - 996	Ind 11 - 20	White Gold Corp. - 100%	Dawson	3/15/2023	10
YC61018 - 039	IND 21 - 42	White Gold Corp. - 100%	Dawson	3/15/2023	22
YC96113 - 124	IND 43 - 54	White Gold Corp. - 100%	Dawson	3/15/2021	12
YC96101 - 112	IND 55 - 66	White Gold Corp. - 100%	Dawson	3/15/2021	12
YC96137 - 162	IND 67 - 92	White Gold Corp. - 100%	Dawson	3/15/2021	26
YC96125 - 136	IND 93 - 104	White Gold Corp. - 100%	Dawson	3/15/2021	12
YC95578 - 579	IND 105 - 106	White Gold Corp. - 100%	Dawson	3/15/2021	2
YC96177 - 200	IND 107 - 130	White Gold Corp. - 100%	Dawson	3/15/2021	24
YC96163 - 168	IND 131 - 136	White Gold Corp. - 100%	Dawson	3/15/2021	6
YF70101 - 104	IND E 1 - 4	White Gold Corp. - 100%	Dawson	4/20/2021	4
YF70121 - 124	IND E 21 - 24	White Gold Corp. - 100%	Dawson	4/20/2021	4
YF70135 - 138	IND E 35 - 38	White Gold Corp. - 100%	Dawson	4/20/2021	4
YF70145 - 148	IND E 45 - 48	White Gold Corp. - 100%	Dawson	4/20/2021	4

Total: 152

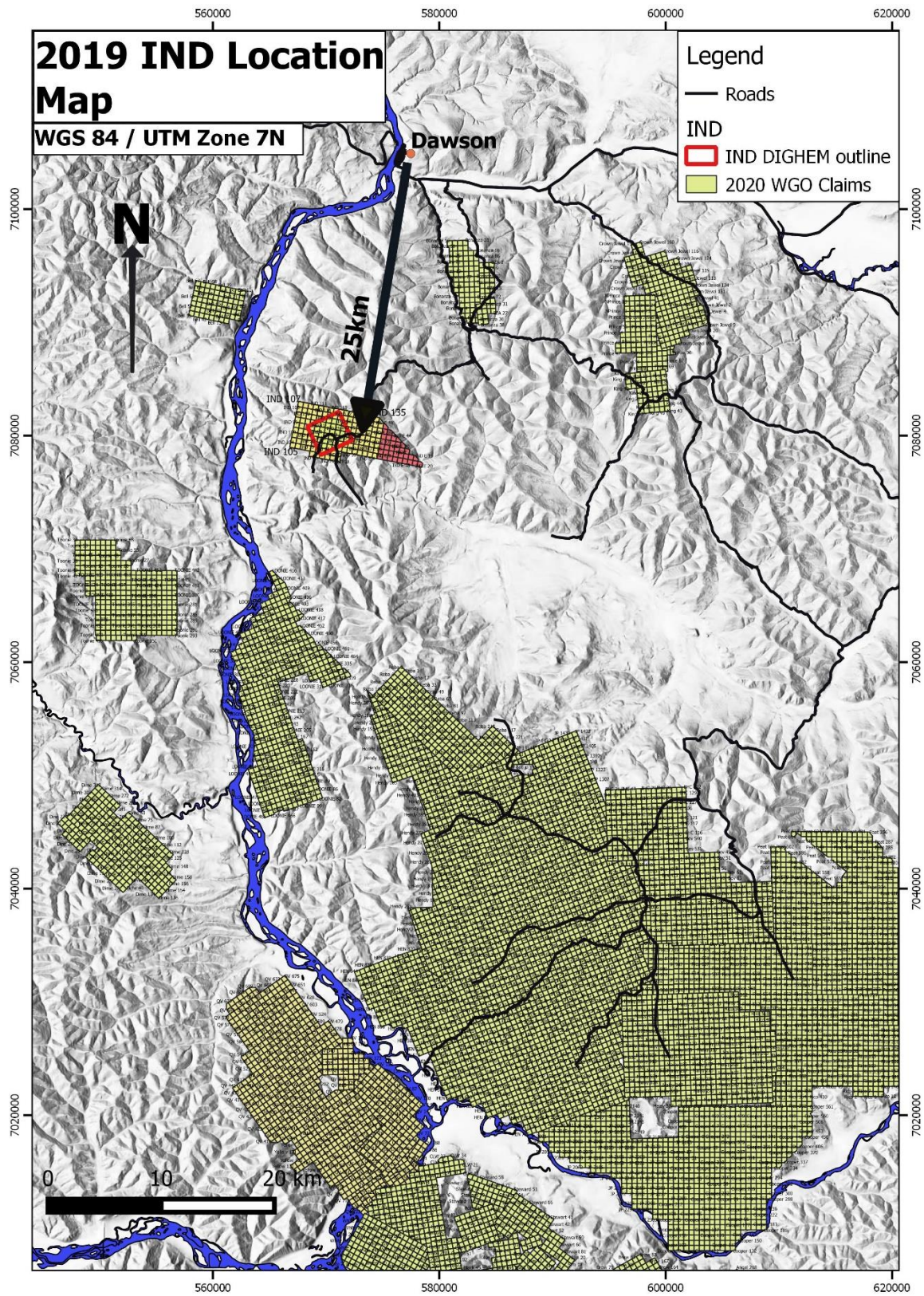


Figure 1: IND Location Map

History and Previous Work

Very little historical work on the immediate IND area is recorded with the Yukon Department of Mines, Energy and Resources. A small drill program (7 holes totaling 189 feet) for Tamark Inc. on Ensley Creek directly north of the IND block is recorded by Beets (1986) but no results are reported.

The first work reported directly on the IND claims is the geophysical and geochemical program described by Ryan (2008). At the time of the work, IND 1 – 42 (see Table 1) were held by Ryanwood Exploration. The rest of the IND block had yet to be staked. Soil sampling in 2005 and 2006 had identified a gold-in-soil anomaly, and the purpose of the 2007 program was to better define and extend this anomaly.

Geophysical work consisted of a ground-based magnetic survey which delineated two broad magnetic highs, the westernmost of which is roughly co-incident with the previously mapped extent of the Jim Creek Pluton. The eastern magnetic high does not coincide with the previously mapped extent of the pluton (Gordey and Ryan 2005), however Ryan (2008) states that the pluton may be more extensive than previously shown, and thus the eastern magnetic high may also represent igneous bedrock. Gold-in-soil anomalies with co-incident lanthanum and bismuth highs are located primarily over these magnetic highs.

This program was followed up with a two-day geological and geochemical evaluation by Jean Pautler, described fully in Pautler (2009). The author produced a 1:7,500 scale map of, and took grab rock samples from, the geochemically anomalous area identified by Ryan (2008). Results confirm that the Jim Creek Pluton has outliers not recorded on the map of Gordey and Ryan (2005). Primarily within the granite but extending into country rock, Pautler (2009) identified minor pyrite, limonite after pyrite, hematite, silicification, sericite alteration and quartz stockwork veining. It was recommended that a trenching and property-wide mapping program be conducted in order to identify promising drill targets. Based on these recommendations, three trenches were excavated and left unfilled.

The 2010 program consisted of geochemical and petrographic analysis of rock samples from two trenches with a total length of 685m. The eastern trench (TR10-4) contained several zones with highly anomalous gold grades (up to 12 g/t over 30 cm and 2 g/t over 10 m), hosted within granite interpreted to be part of the Jim Creek Pluton. Six samples were submitted for petrographic analysis, showing evidence of hydrothermal alteration both within the granite of the pluton and in the country rock.

The 2011 exploration program consisted of 7 diamond drill holes totaling 1316.73m. Sporadic low-grade Au samples were intercepted with 4 samples >1 g/t Au (max 2.44 g/t Au); the best intercept was 0.56 g/t Au over 13.5m from 19.6m depth in IND11-05.

The 2013 work program consisted of 581 soil samples and 20 GT Probe samples. The 2014 work program consisted of 82 soil samples and 59 GT Probe samples. The 2016 work program consisted of 183 GT Probe samples.

In 2017 White Gold Corporation commissioned Groundtruth Exploration Ltd. of Dawson, Yukon to perform Rotary Air Blast (RAB) Drill, Reverse Circulation (RC) Drill, GT Probe, Soil Sampling, IP Survey, Dighem and drone aerial survey programs on their IND Gold Property. 359 Soil samples, 15 IP profiles (6.225 line km), 172 GTProbe samples, 4 RAB holes (140.2m), 5 RC holes (486.15m), 40km² of Drone survey (12cm resolution) and 87 line km of Dighem were collected on the property during the 2017 field program (the Dighem survey was contracted to CGG Global of Toronto).

Geology

Regional Geology

The Property is in the Stewart River-Klondike goldfield area within the Yukon-Tanana Terrane (YTT). The basement rocks in this region are pervasively foliated and recrystallized schists and gneisses, which have metamorphic grades ranging from greenschist facies in the north to amphibolite facies on the BHC Property. Three generations of plutonism (Devonian, Mississippian, and Permian) are recognized in the Stewart River area. Granitoids and basement rocks have developed two discernable metamorphic foliations. Compression during the Jurassic resulted in the development of narrow shear zones and thrust stacking of lithologic units. During the Cretaceous the regional stress field shifted to extensional and normal faults oriented north-south and east-west developed. These faults controlled the emplacement of Cretaceous and early Tertiary intrusions. As this system evolved into the Eocene, extension was accommodated by transcurrent slip along the Tintina Fault (Figure 2).

The region underwent ductile (D1/D2) deformation associated with amphibolite facies metamorphism during the Late Permian Klondike orogeny. This event was associated with the accretion of the YT to Laurentia and associated closure of the Slide Mt Ocean and obduction of ophiolitic slices of the Slide Mt terrane. The area underwent additional compression and ductile deformation (D3) associated with greenschist facies metamorphism during the Late Triassic-Early Jurassic. The event was associated with widespread thrust faulting and imbrication of the Slide Mt. terrane, and the emplacement of felsic to ultramafic intrusions. This transitioned into a period of regional uplift and exhumation and is associated with dominantly east-west oriented sinistral faults, localized north-northwest vergent folds, and high angle reverse faults (D4). This period of deformation spans the ductile to brittle transition and are associated, particularly the E-W sinistral faults, with 'orogenic' style gold mineralization throughout the White Gold district and Klondike. Figure 3 below shows a correlation chart for the major tectonic, structural, magmatic, and mineralizing events in the west-central Yukon and eastern Alaska.

Renewed northeast dipping subduction under the continental margin during the Late Cretaceous led to renewed magmatism across the YT and is associated with felsic to intermediate intrusions of the Dawson Range batholith and felsic-mafic volcanic rocks of the Mount Nansen suite. The Early Cretaceous arc activity ceased around 99Ma; at which point it stepped farther inboard and is associated with intrusive suites in the Selwyn Basin (ie. Tombstone suite, etc.). This lull in magmatism was associated with the formation of the Indian River Formation, a coarse clastic sedimentary package deposited in an

alluvial/fluvial to shallow marine setting that records approximately 40 million years of sedimentation following the formation of the Dawson Range Arc.

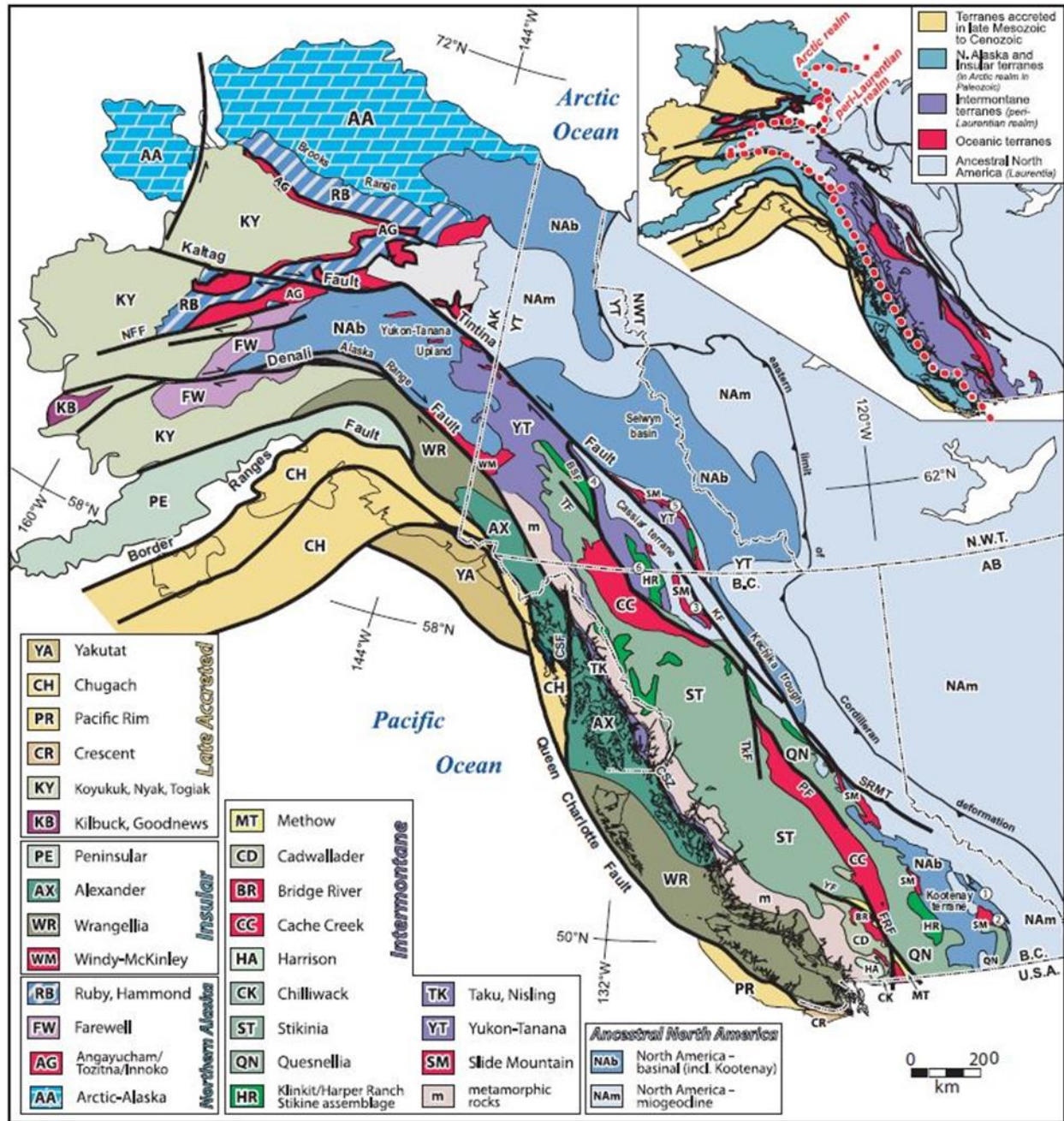


Figure 2: Regional Geology Map

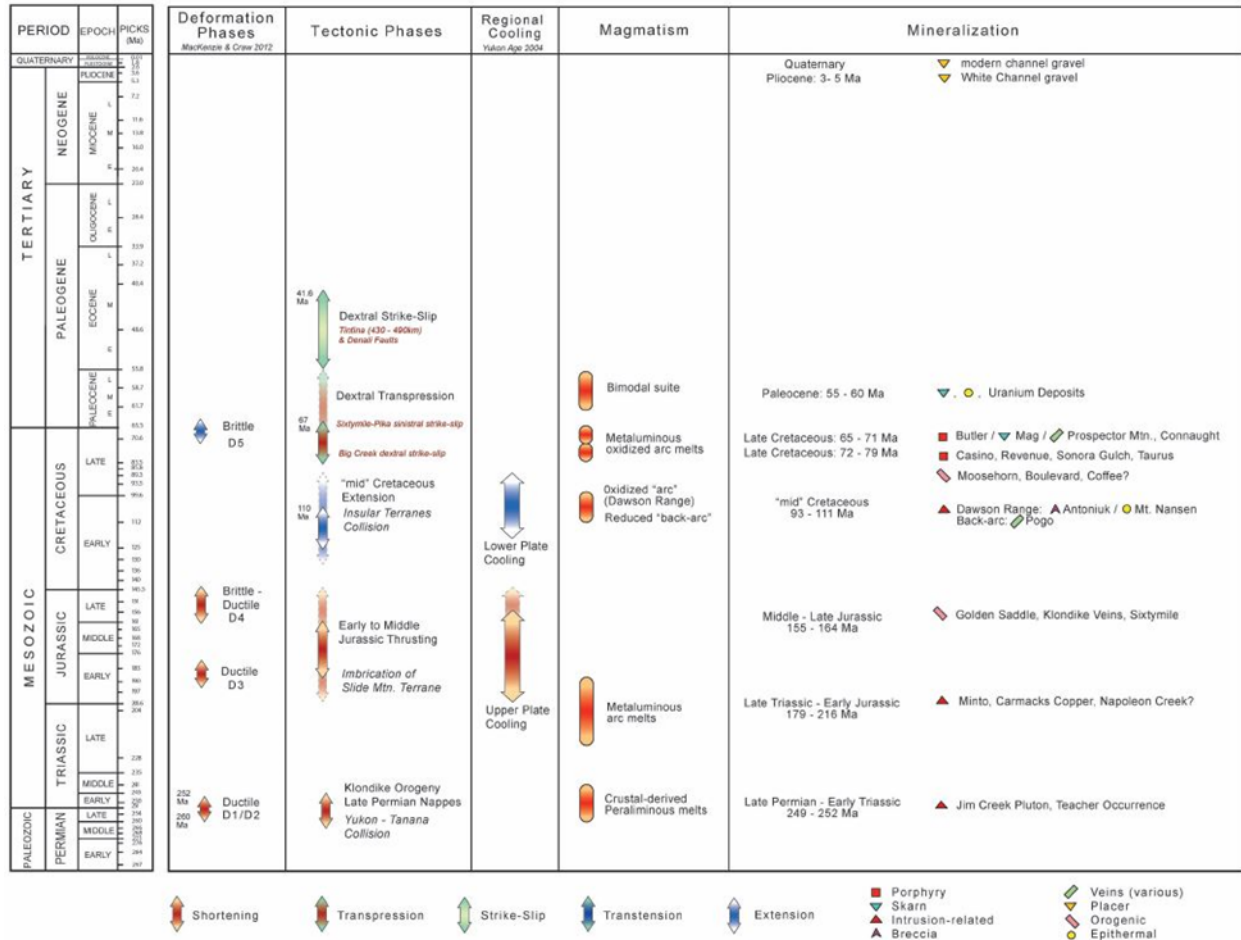


Figure 3: Correlation Chart of Major Geological Events - YT, AK

Arc style magmatic and volcanic activity renewed during the Late Cretaceous and is associated with a series of calc-alkaline plutons and high-level porphyry dikes, plugs, and breccias in the Casino and Freegold areas, and age equivalent intrusions in eastern Alaska (79 – 72Ma). This event was also likely associated with the initiation of dextral offset along the Big Creek fault and reactivation of older Jurassic age structures in Dawson Range area. It is also associated with variable styles of mineralization ranging from Cu-Au-Mo porphyries (Casino), intrusion-related/epithermal occurrences (Sonora Gulch, Freegold area), and structurally controlled gold / 'orogenic' mineralization (Coffee, Boulevard, Moosehorn). At 72Ma there was a distinct change in magmatism with widespread bi-modal volcanism (Carmacks group) and the emplacement of small, high-level, felsic plugs and stocks (Prospector Mountain suite) throughout the YT. A prominent set of northeast trending normal and sinistrally oblique faults are commonly associated with the intrusive and volcanic rocks of this event and are broadly coeval with magmatism.

A final magmatic event occurred during the Late Tertiary and is associated with the emplacement of bi-modal suite of predominately north-south trending dike swarms, plugs, and local pyroclastic rocks. Gabrielse et al 2006 suggests that the magmatic event was likely coeval with the early stages of dextral offset along the Tintina fault (Gibson, 2014).

Property Geology

Underlying the IND claim block itself (Figure 4) are quartzite, metapelite and marble of the Devonian-Mississippian Nasina Assemblage intruded by the ~252 Ma Jim Creek Pluton, a coarse-grained unfoliated biotite-bearing granite to quartz monzonite (Gordey and Ryan 2005).

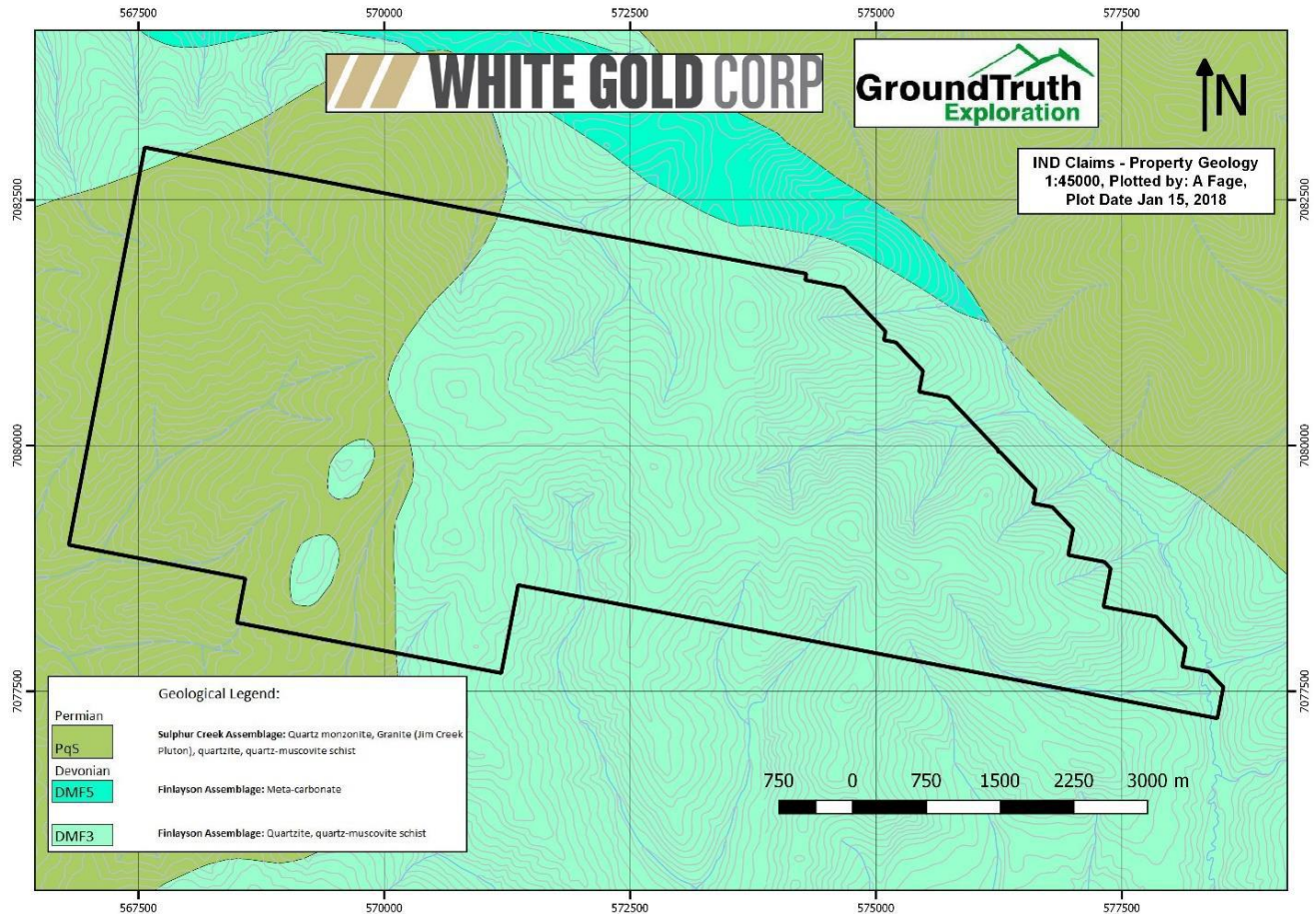


Figure 4: Property Geology Map

2020 Geophysical Interpretation

The interpretation covers the entire IND property using historic aerial mag and radiometric data. It also uses data from the 2017 8.5km² aerial DIGHEM survey and IP survey's (Figures 5 and 6).

Methods and Procedures

Methods and Procedure can be found in the "IND Geophysical Report" by Amir Radjaee, Ph.D., P.Geo. in Appendix I.

Analysis

Refer to Airborne Geophysical Report in Appendix I to gather analysis information.

Results and Interpretation

Most of the conductive zones are associated with low resistivity (high conductivity) areas identified by 3D inversion modelling of DCIP data. Some high chargeability anomalies overlie high gold areas, mostly near the edges of low resistivity zones (Figure 6). The EM results define a pronounced E-W trending conductor mapped from EM in-phase and quadrature waveforms at different frequencies. These conductors are sub-parallel with the magnetic lineaments mapped from aeromagnetic data and correlate well with the general trend of the gold in soil geochemical anomalies. See the report in Appendix I for more details and figures.

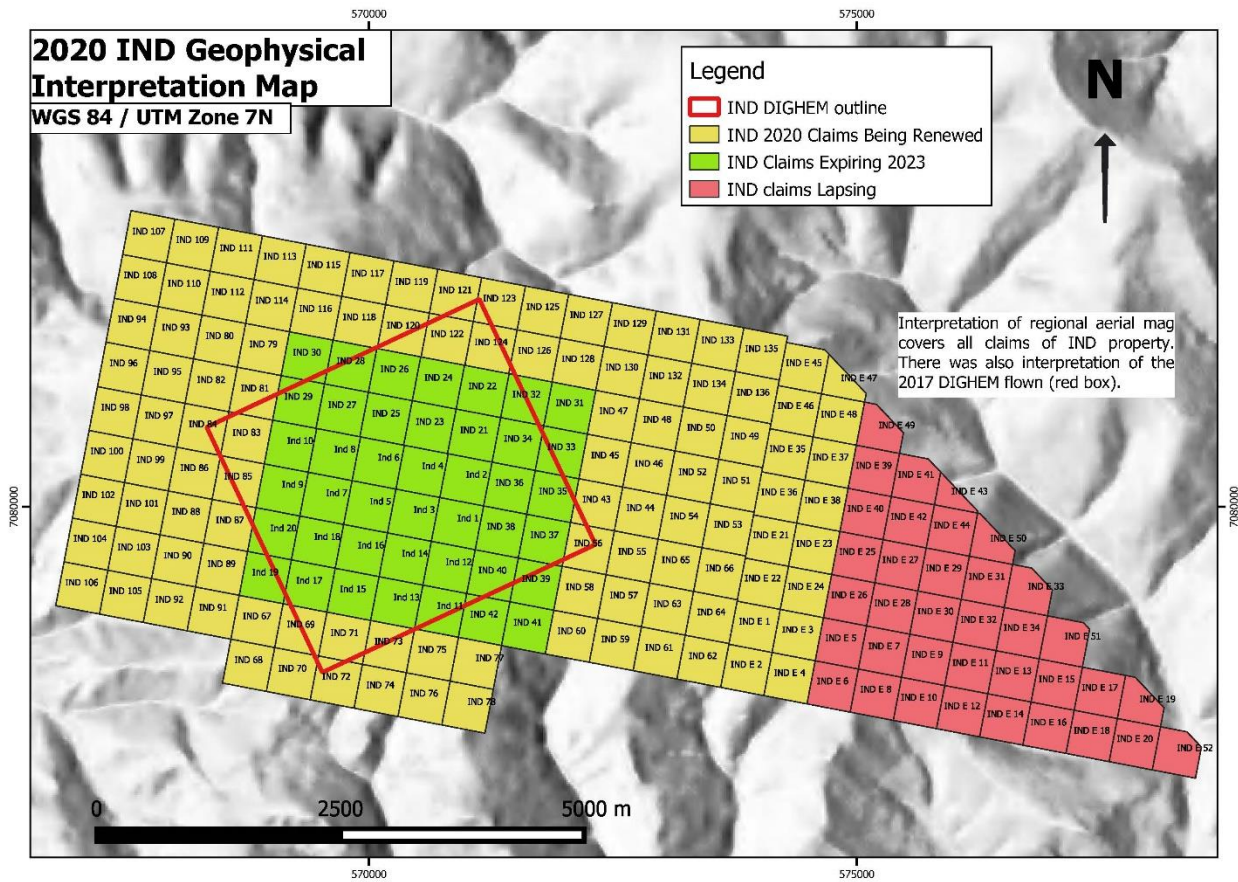


Figure 5: Claims Map and DIGHEM area

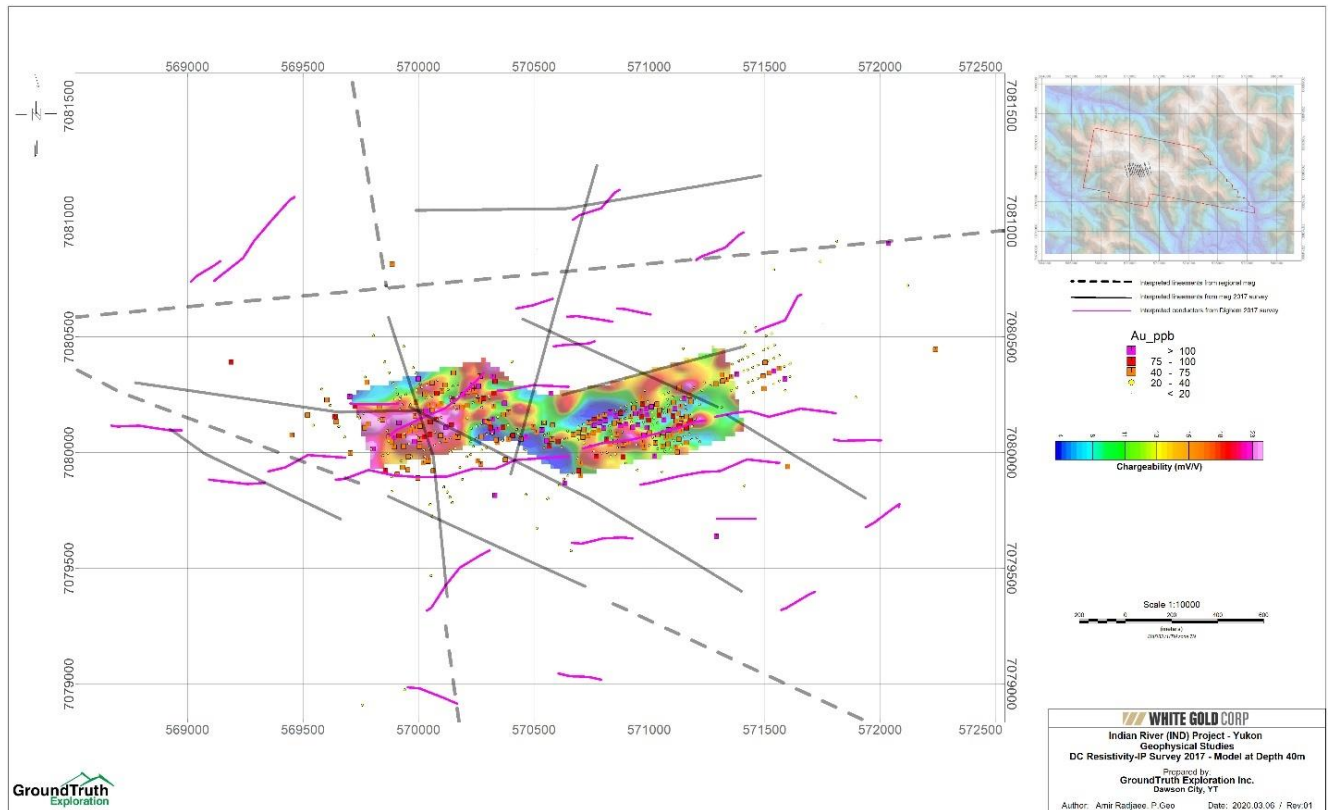


Figure 6: Chargeability at 40m depth with overlying Au in soil

References

Allan, M. M., Hart, C. J., & Mortensen, J. K. (2013). Magmatic and metallogenic framework of west-central Yukon and eastern Alaska. *Jurnal Name*, 1-13.

CGG Canada Services, SURVEY REPORT, 2017, Airborne magnetic and DIGHEM survey, PROJECT# 602997

Colpron, M., Israel, S., Murphy, D., Pigage, L. and Moynihan, D., 2016. Yukon Bedrock Geology Map. Yukon Geological Survey, Open File 2016-1, 1:1,000,000 scale map and legend.

Deklerk, R. and Traynor, S. (compilers), 2005. Yukon MINFILE 2005 - A database of mineral occurrences. Yukon Geological Survey

Fage, A., Hanlon, J., Radjaee, A., 2018. Geochemical, Geophysical & Airborne Survey Assessment Report: Rotary Air Blast (RAB) Drill, Reverse Circulation (RC) Drill, GT Probe, Soil Sampling, IP Survey, Dighem & Drone aerial survey. Dawson, Yukon. GroundTruth Exploration.

GeoSci Developers, 2017, Geophysics for Practicing Geoscientists.

Gordey, S.P. and Makepeace, A.J. (comp.) 2003. Yukon digital geology, version 2.0; Geological Survey of Canada Open File 1749 and Yukon Geological Survey Open File 2003-9(D)

Gordey, S.P. and Ryan, J.J. 2005. Geology, Stewart River Area (115N, 115O and part of 115J), Yukon Territory; Geological Survey and Canada, Open File 4970, scale 1:250,000.

Mortensen, J.K. 1992. Pre-mid-Mesozoic tectonic evolution of the Yukon-Tanana terrane, Yukon and Alaska. *Tectonics*, 11: 836 – 853.

Pautler, J. 2009. Technical Report on the Indian River Project, Dawson, Yukon Territory. 2017

Ryan, Shawn. 2008. Geophysical-geochemical report, IND claims. Yukon Mines, Energy and Resources Report YMIP 2007-047.

Swanton, D., Equity Exploration Consultants, 2011. 2010 Geochemical Report on the IND Project

USGS, 1999, Geologic Interpretation of DIGHEM Airborne Aeromagnetic and Electromagnetic Data over Unga Island, Alaska.

Statement of Expenditures

Description	Amount
March 15/20 - Evaluation Report on IND Property Geophysics Compilation (preapproved by Dawson Recorder on Feb 26/20)	
1. Evaluation Report on IND Geophysical Data- Amir Rajae Comprehensive Compilation, Modelling and Interpretation March 1-11, 2020 - 10.5 days Charged at Consulting Rate of \$1050/day, including all processing software	\$11,025.00
GST # 811084268 RT0001	
Subtotal	\$11,025.00
GST 5%	\$551.25
Thank you for your business!	
Total Due	\$11,576.25

Statement of Qualifications

I, Matthew Hanewich, do hereby declare that:

1. I am currently assisting with end of season report writing for GroundTruth Exploration Inc. of Dawson City, Yukon.
2. I graduated from Carleton University in 2015 with a B.Sc. Honor's degree in Geology.
3. I have worked as a geologist on and off since 2014.
4. I am not aware of any material fact or material change with respect to the subject matter of this report, the omission to disclose which makes this report misleading.

Dated this 7th day of April 2020

Matthew Hanewich

White Gold Corp.

COMPILATION, PROCESSING AND INTERPRETATION OF GEOPHYSICAL DATA

IND Property, YT

Work Performed On: February 24 to March 14, 2020

Prepared By:

GroundTruth Exploration Inc.
BOX 70, Dawson City, YT, Y0B 1G0

March 14, 2020

Author: Amir Radjaee, *Ph.D., P.Geo.*
Report #: WGO-IND-REG2020-01

Executive Summary

The IND property is located Yukon's Klondike district, approximately 25km south of Dawson City, in the Dawson Mining District on NTS map sheet 115O/13, 14 and is owned by White Gold Corp. The center of the property is situated at UTM coordinates 572,000E 7,080,000N (NAD 83, UTM Zone 7).

The GroundTruth Exploration has completed compilation, levelling and merging of all available aeromagnetic, DC Resistivity IP, and airborne EM datasets within the identified area of interest for the IND property. The modelling efforts consisting of 3D unconstrained inversion of regional and property scale magnetic, 2D and 3D inversion of DC Resistivity IP, and 1D laterally parameterized inversion modeling of airborne EM datasets. This work considers all geophysical data available for the project area.

The inversions were performed using the UBC-GIF MAG3D, EM1DFM, suite of algorithms for the magnetic and AEM data respectively as well as RES2DINV and RES3DINV for DC Resistivity IP data. The products are 3D inversion models of magnetic susceptibility, electrical conductivity and chargeability, and integrated products combining the individual physical property models.

The interpretation of lineaments as well as the conductive features provide guidance to the regional structures, prospective geology and location of possible alteration and mineralization zones. This work was performed from February 24 to March 13, 2020 and was undertaken on behalf of White Gold Corp.

The extensive set of digital deliverable products that accompany this presentation report include physical property models, cut-off iso-surfaces, section and horizontal grids, maps, shapefiles, and the inversion models in several different commonly used formats.

Table of Contents

1.0	Introduction	5
2.0	Compilation of airborne magnetic data	6
3.0	3D unconstrained inversion modeling of mag data	9
4.0	1D inversion modeling of EM data	16
5.0	Unconstrained 2D/3D inversion modeling of DCIP data	18
6.0	Integration of data and Interpretation	21
7.0	Conclusions and Recommendations	27
8.0	Submittal	29
9.0	Deliverables	29
10.0	References	30
11.0	Statement of Qualifications	31
	Appendix A	32

List of Figures

Figure 1: The outline of claim boundary for IND project.	5
Figure 2: Layout of flight lines for the regional airborne magnetic survey.....	7
Figure 3: The magnetic RTP grid for regional and property scale data	8
Figure 4: Observed and predicted data from the recovered regional sus. model	10
Figure 5: The 3D Regional magnetic sus. for forward modeling.....	12
Figure 6: Original magnetic field and corrected data after regional removal	12
Figure 7: Observed and predicted data from the recovered detailed sus. model.	13
Figure 8: The horizontal slice at 800m ASL for regional magnetic sus. model.	14
Figure 9: The horizontal slice at 700m ASL for detailed of magnetic sus. model.	15
Figure 10: 3D view of high magnetic sus. areas.....	15
Figure 11: The resistivity depth slice at 40m extracted from interpolated 3D model. ...	17
Figure 12: 3D view of conductive zones greater than 0.002 moho.....	18
Figure 13: Resistivity depth slice at 40m surface from 3D inversion of DCIP.....	19
Figure 14: Chargeability depth slice at 40m surface from 3D inversion of DCIP.	20
Figure 15: Low resistivity and high charg. iso-surfaces from 3D inversion of DCIP.	20
Figure 16: The RTP magnetic residual and interpreted lineaments	22
Figure 17: Magnetic RTP for regional and 2017 AMagc survey 2017	23
Figure 18: Resistivity depth slice at 40m from inversion modelling of Dighem 2017	24
Figure 19: Resistivity depth slice at 40m from Dighem and DCIP 2017 surveys.....	25
Figure 20: The chargeability at 40m with interpreted lineaments conductors.....	26
Figure 21: Gold assay grid from soil geochemical data and geophysical models	27

List of Tables

Table 1: The regional scale datasets used for compilation.	8
Table 2: Regional inversion modelling specifications.....	10
Table 3: Inversion modelling specifications for the IND property detailed inversion.	13

1.0 Introduction

Geophysical prospecting methods used in exploration provide information about the physical properties of the subsurface. These properties can, in turn, be interpreted in terms of lithology and/or geological characteristics of deposits. Moreover, the geometric distribution of physical properties can help delineate geological structures and may be used as an aid in determining mineralization and subsequent drilling targets.

The IND property has a long history of various methods of Geophysical survey work undertaken. These surveys include 2017 airborne FDEM (Dighem) and magnetic, and DC resistivity-IP surveys.

White Gold Corp. is planning to re-evaluate the geophysical work done by compiling and reprocessing all data available with modern inversion and modelling software tools, integration and interpretation of results. The report will prepare recommendations for tested and untested exploration targets and assess the suitability of geophysical used methods historically to determine the best methods moving forward. The outline of the claim boundary is shown in Figure-1.

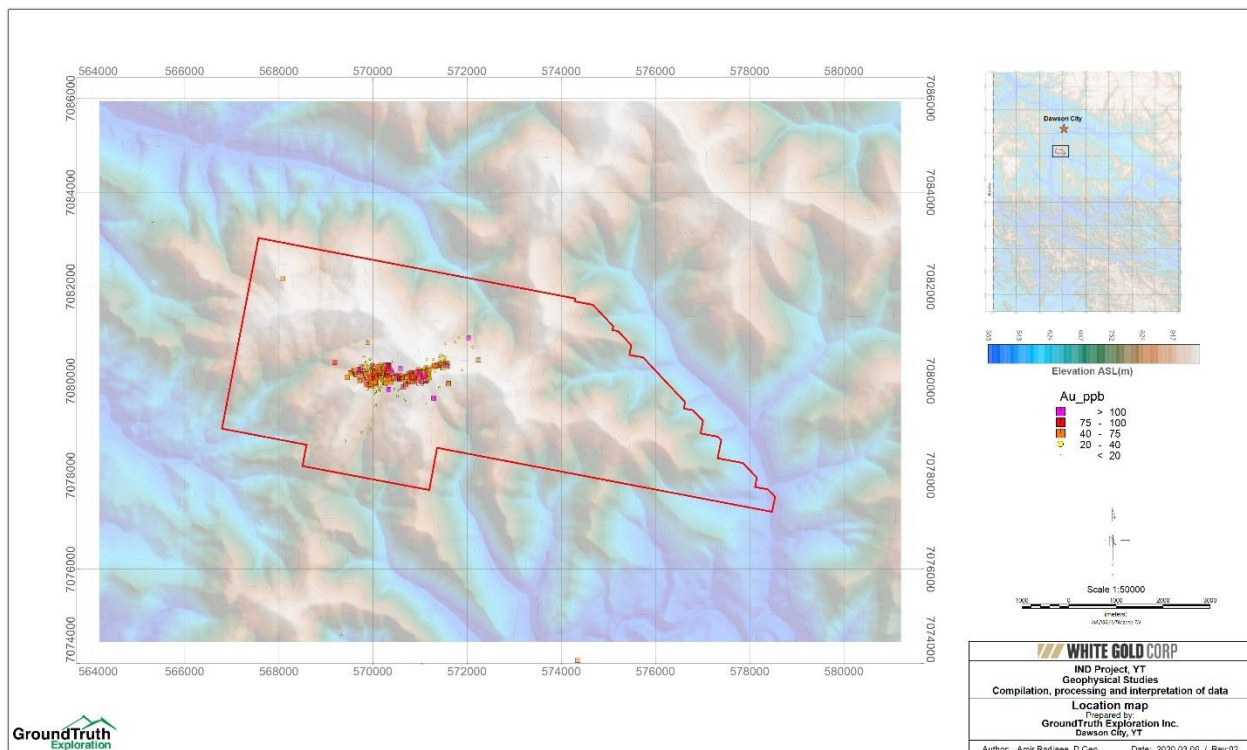


Figure 1: The outline of claim boundary for IND project, YT.

2.0 Compilation of airborne magnetic data

Magnetic anomaly maps are one of the essential tools for mapping surficial and buried rocks, for determining the geologic structure, and for discovering some types of mineral deposits. Regional geologic features may become more evident after individual aeromagnetic surveys are compiled and plotted at the same scale in a consistent way.

The GroundTruth Exploration has completed compilation, levelling and merging of all available high-resolution aeromagnetic datasets within the area of interest identified for the regional studies of IND project into usable wholes. The results provide guidance to the regional structures, prospective geology and location of possible alteration and mineralization zones.

The available and downloaded datasets for this project consist of about 10 distinct aeromagnetic surveys collected at different times, elevations and line spacings. All data were provided or transformed to the NAD83 UTM Zone 7N Datum and coordinate system. Topographic data were obtained from the White Gold Corp. on a 15m grid. This topography surface was used as a reference for levelling of all airborne magnetic data. The data processing was carried out in the same coordinate system. The available datasets are organized into two groups as follows:

- Regional scale airborne magnetic data, a total of 2 datasets
- Property scale high-resolution aeromagnetic data, a total of 8 datasets

The survey parameters of datasets that have been used for compilation and levelling are summarized in Table-1. The outline of the area of interest for regional study, claim boundaries and layout of survey flight lines for the airborne magnetic survey are shown in Figure-2.

The software programs used for data preparation and processing include Geosoft and USGS extension GX modules. For levelling and compilation of aeromagnetic datasets into a regional scale, the below data processing sequences was performed for all datasets throughout the project.

- Data QC/QA, inspection and analysis of geophysical and spatial data, edit of the database for bad data points, down-sampling
- Checking the survey parameters for each survey block, extracting the geomagnetic ambient field parameters to calculate Reduced to Pole (RTP) field
- Continuation transformation and 2D grid processing of RTP, filtering, and decorrugation if required

- Leveling of RTP data by using appropriate processing approach depending on the quality of data such as tie-line correction, virtual tie-line, etc.
- Compilation of leveled data and adjustments, creating derivative grid products, review of processing steps if required

All data were imported into Geosoft. Data were examined and edited for bad data points. The ambient magnetic field including declination, inclination, and International Geomagnetic Reference Field (IGRF) was computed for each survey block. The magnetic data were upward continued to a datum surface and corrected for the DC shifts (if needed) before levelling.

Figure-3 shows the magnetic RTP for regional compiled data and property scale compiled data after leveling and merging.

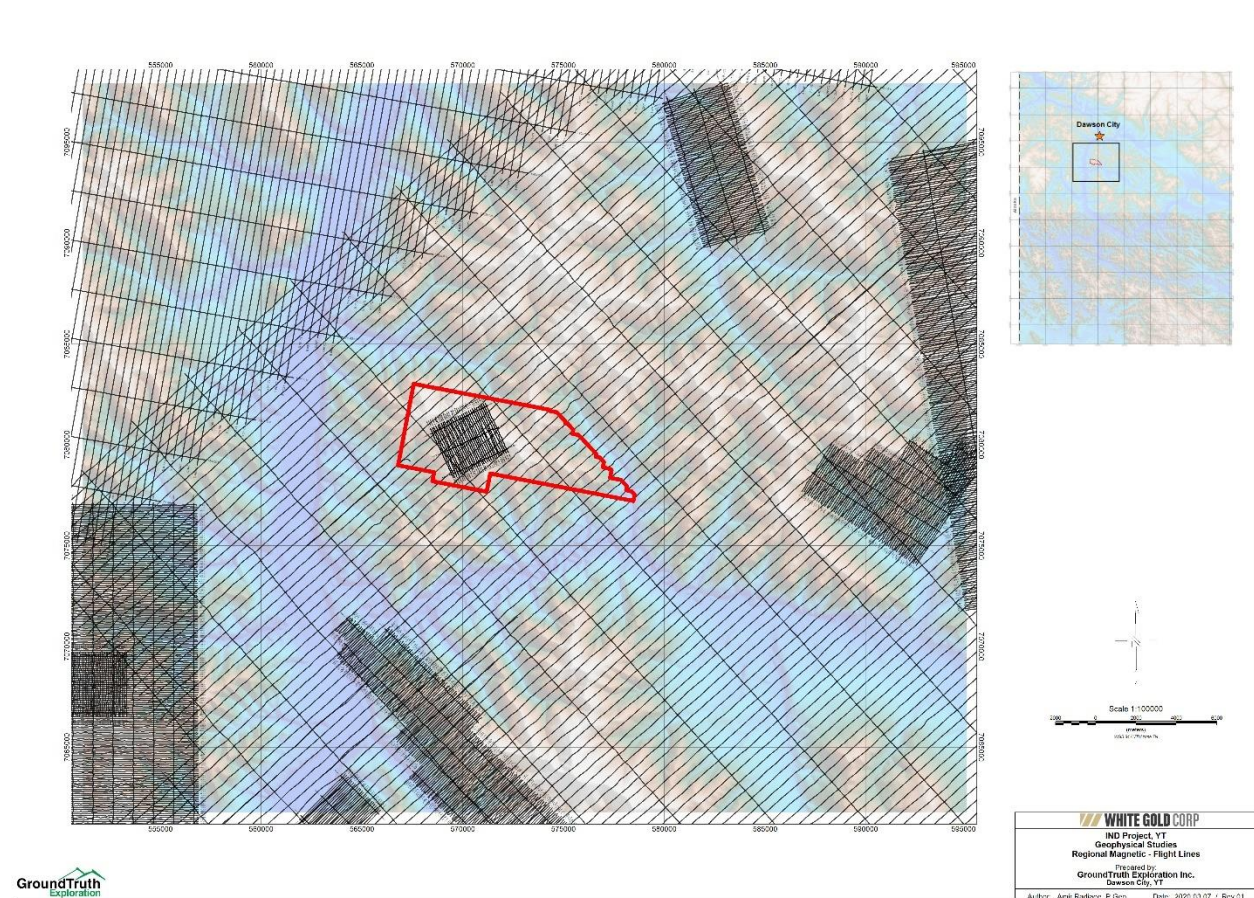


Figure 2: Layout of flight lines for the regional airborne magnetic survey.

Table 1: The regional scale datasets used for compilation.

No.	Survey Block	Year	Line direction	Line Spacing	Survey Type
1	Stewart River I	2000	SW-NE (N 048°)	500m	Regional Scale
2	Dawson	2014	SW-NE (N 10°)	400m	Regional Scale
3	YGS-95963 DanTaku Reba	2010	SW-NE (N 45°)	100m	Property Scale
4	YGS-95964	2010	SW-NE (N 33°)	100m	Property Scale
5	YGS-94021	1999	SW-NE (N 80°)	100m	Property Scale
6	Toonie	2011	E-W (N 90°)	100m	Property Scale
7	602997_Dighem-03	2017	N-S (N 0°)	100m	Property Scale
8	602997_Dighem-06	2017	NE-SW (N 225°)	100m	Property Scale
9	602997_Dighem-08	2017	NW-SE (N 335°)	100m	Property Scale
10	602997_Dighem-09	2017	NE-SW (N 254°)	100m	Property Scale

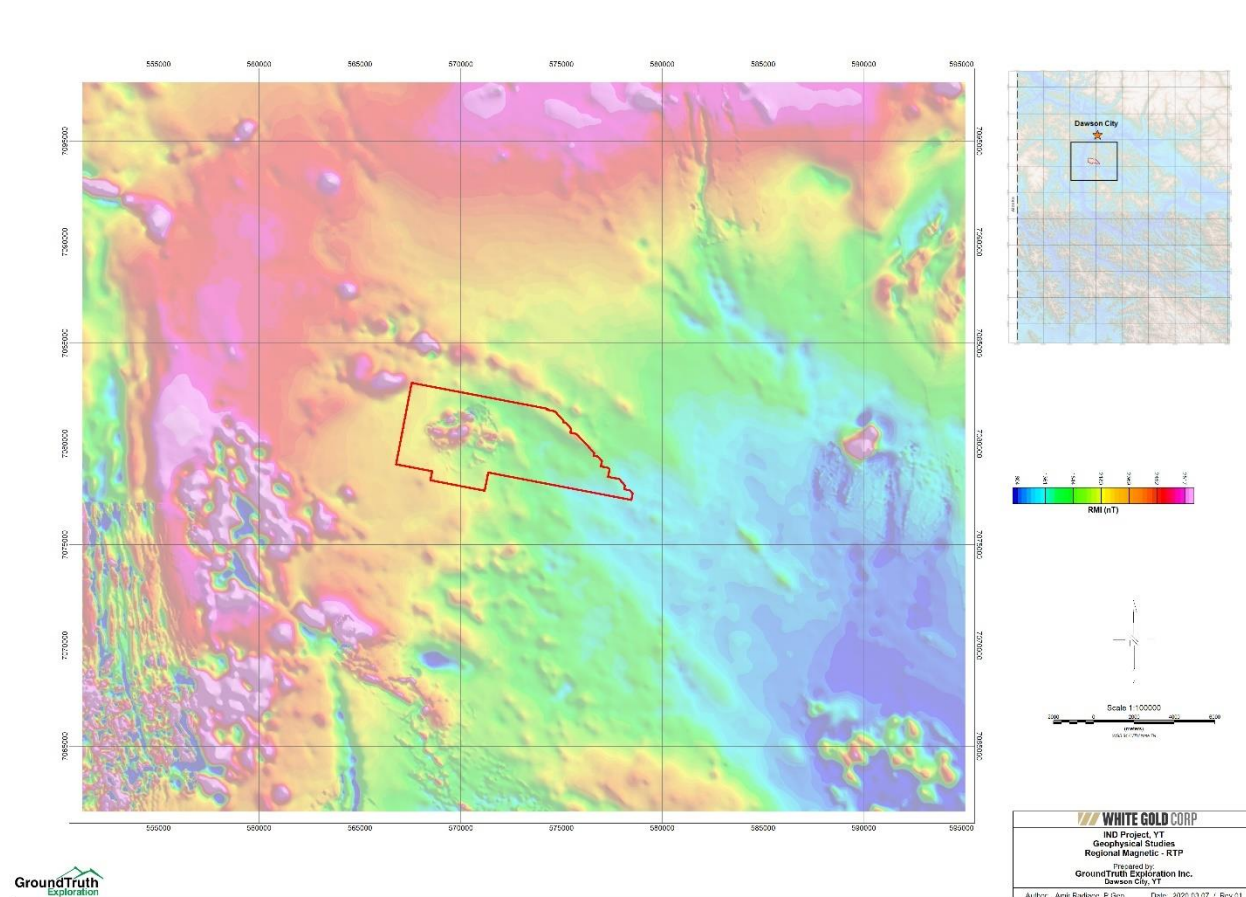


Figure 3: The magnetic (reduced to pole) RTP grid for regional and property scale compiled data after leveling and merging.

3.0 3D unconstrained inversion modeling of mag data

Magnetic Total Field data are inverted for a 3D susceptibility model of the earth using the UBC-GIF MAG3D inversion code. The assumption has been made that no self-demagnetization or remanent magnetization effects exist. The topography is included in the inversions. The ambient magnetic field parameters are needed for inversion modeling and computation of the Reduced-to-Pole (RTP) magnetic anomaly which are calculated by MAGMAP extension module of Geosoft for all data points.

3D inversion modelling has been performed using a discretized 3D earth, which employs many fine cells, each of which has a constant physical property value. The discretization is in the form of cuboid cells for the 3D magnetic inversions and is commonly referred to as a mesh. The mesh parameters are based on the survey and system parameters and are made small enough to reduce modelling errors due to discretization and are also small enough so that they do not introduce additional regularization in the inverse problem.

The 3D model has a core mesh of regularly sized cells corresponding to the lateral extents of the data. Padding cells of increasing dimensions extending east, west, north, south, and vertically down complete the volume used in the inversion. The padding cells help accommodate signals that cannot easily be accounted for the core mesh. Padding cells are removed for deliverable model products.

The RTP magnetic field after compilation, levelling and merging of data is used for the regional inversion. The magnetic data were upward continued to a datum 200m above the flight surface before inversion. Regional 3D magnetic inversion modelling used a coarse discretization with cell sizes of 500m x 500m x 100m.

A standard deviation equivalent to 2% of the magnetic field was assigned to the data. The data were prepared in the UBC ASCII data format for inversion modelling. The coefficients for each model component is computed from corresponding length scales. The inversion modelling parameters for regional modelling are presented in Table-2. Observed and the predicted data from the recovered magnetic susceptibility model are shown in Figure-4.

Table 2: Regional inversion modelling specifications.

Inversion Modelling Parameters	Inversion Modelling Parameter Value
Convergence Criteria	Chi-factor = 1
Coefficients for each model component	$a_s = 4.5E-07$, $a_x = a_y = 1.0$, $a_z = 4.00E-2$
Number of data inverted	317,397
Ambient magnetic field vector	Inclination = 90°, Declination = 0°, Inducing Field Strength = 57,017 nT
Number of cells	102 x 86 x 83= 728,076
Global Susceptibility Bounds	Lower bound=0 SI, Upper bound=1 SI

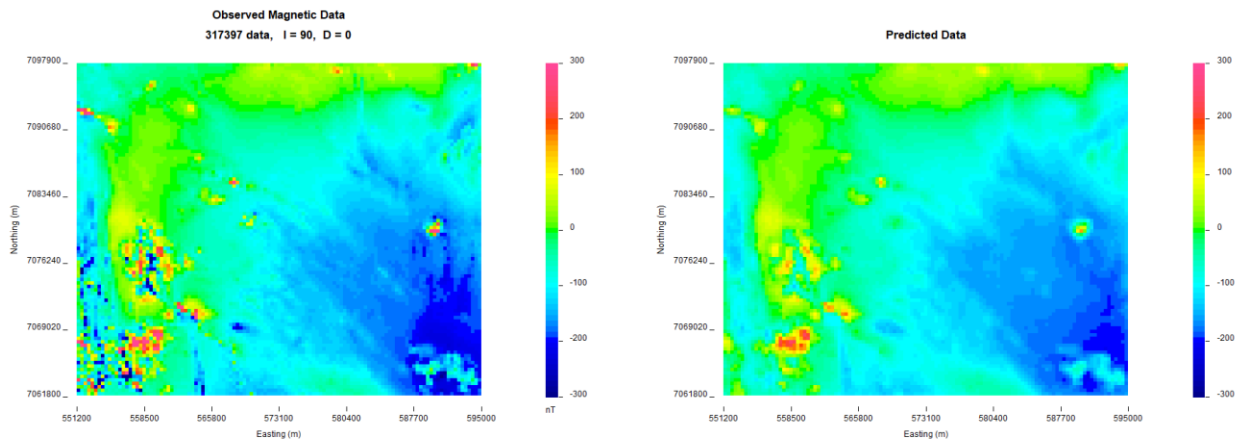


Figure 4: Observed magnetic data (Left) and predicted data from the recovered regional susceptibility model (Right).

A method for separating regional and residual magnetic fields using an inversion algorithm was applied to data prior to the detailed inversion of the IND project magnetic data. The separation is achieved by using a regional susceptibility model out of inversion results of regional magnetic data. The local volume of detailed 3D inversion block is removed from the regional model (model cell values in that volume are set to 0), and the

magnetic fields are calculated by forward modelling used as the regional field. The residual data are obtained by subtraction of the regional field from the original data.

These residual data reflect the response from local and shallower geology that are often dominated by stronger regional sources, and they can be subsequently inverted on the local volume of interest (usually with a more detailed model discretization). The residual data may also be useful for qualitative interpretation of geology within the volume of interest. This modelling-based approach to regional signal removal provides a robust result that is consistent with the modelling objectives. The modelling workflow for separation of the regional signal is outlined as follows:

- Regional Inversion: Invert the entire dataset using a coarse mesh to produce a regional model.
- Regional Response: Define a local volume of interest. Set the magnetic susceptibility value to zero inside this volume and forward model to obtain the regional response.
- Regional Removal: Calculate a residual by subtracting the regional response from the original data.
- Detailed, local Inversion: Invert the residual data using a refined mesh over the local volume of interest.

By calculating a regional response for local volumes of interest, a separate local inversion can be performed on the residual dataset. The regional susceptibility model with zero values for the local block of inversion for IND property is shown in Figure-5. Magnetic Field Intensity before and after regional removal are shown in Figure-6.

The data for IND property were collected between June 8 and July 7, 2017, after removing the regional signal were used for detailed inversion modelling (Figure-6, Right). Detailed local inversions used a more finely discretized 3D mesh with 25m x 25m x 20m cell dimension for the IND property.

A standard deviation equivalent to 2% of the magnetic field was assigned to the airborne magnetic data. The data were prepared in UBC ASCII data format for inversion modelling.

The coefficients for each model component is computed from corresponding length scales. The inversion modelling parameters for regional modelling are presented in Table-3. Observed and the predicted data from the recovered magnetic susceptibility model are shown in Figure-7.

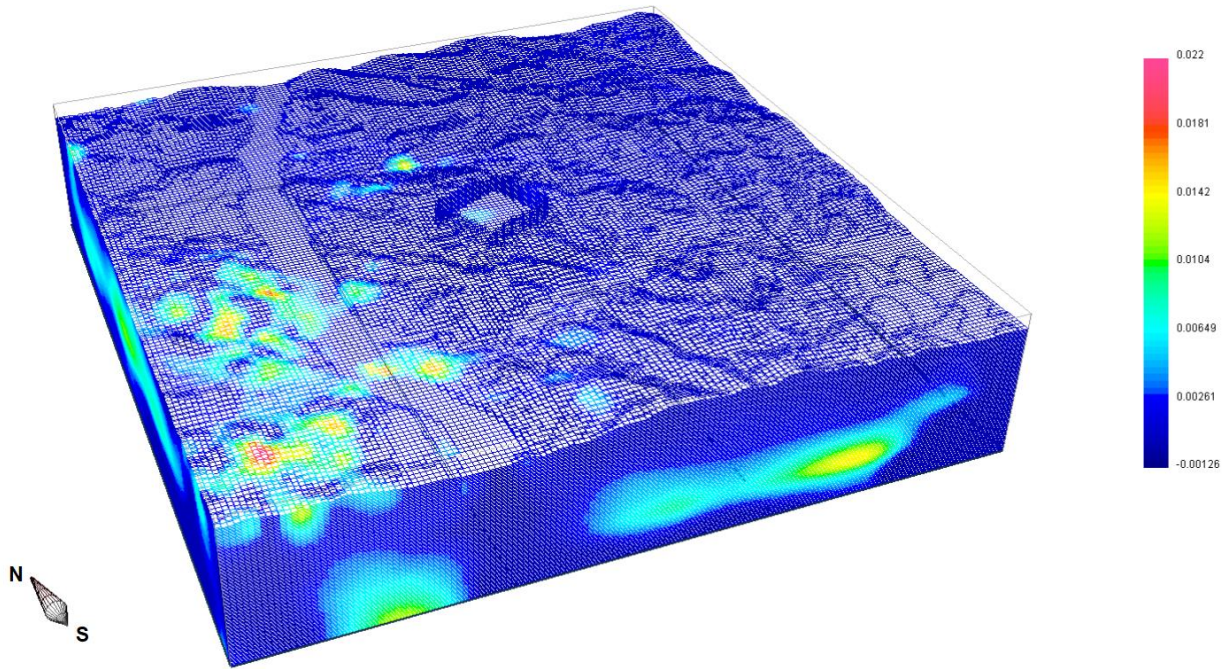


Figure 5: The 3D Regional magnetic susceptibility model with magnetic susceptibility value of inside of the local grid set to zero. The regional response is computed by forward modeling of this model over the observation points of property scale data.

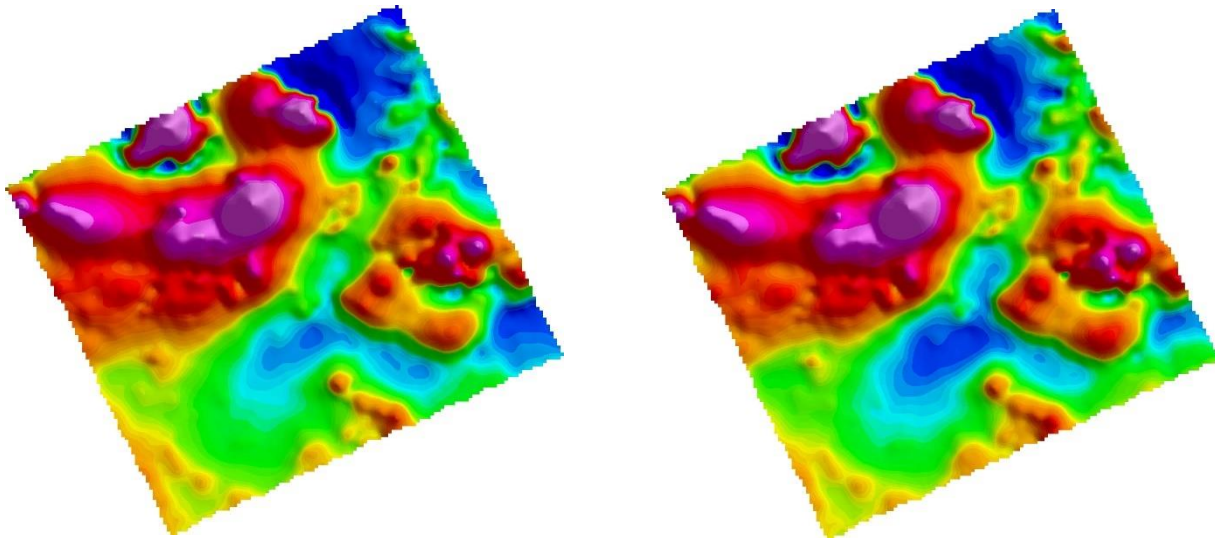


Figure 6: Original magnetic field data (RTP) for the IND 2017 airborne magnetic survey (Left), and corrected data after removing the regional signal by forward modeling of regional sus model (Right).

Table 3: Inversion modelling specifications for the IND property detailed inversion.

Inversion Modelling Parameters	Inversion Modelling Parameter Value
Convergence Criteria	Chi-factor = 2
Coefficients for each model component	$\alpha_s = 1.78E-04$, $\alpha_x = \alpha_y = 1.0$, $\alpha_z = 6.4E-2$
Number of data inverted	13,514
Ambient magnetic field vector	Inclination=90°, Declination =0°, Inducing Field Strength = 57,017 nT
Number of cells	172 x 164 x 108 = 3,046,464
Global Susceptibility Bounds	Lower bound=0 SI, Upper bound=1 SI (min, max)

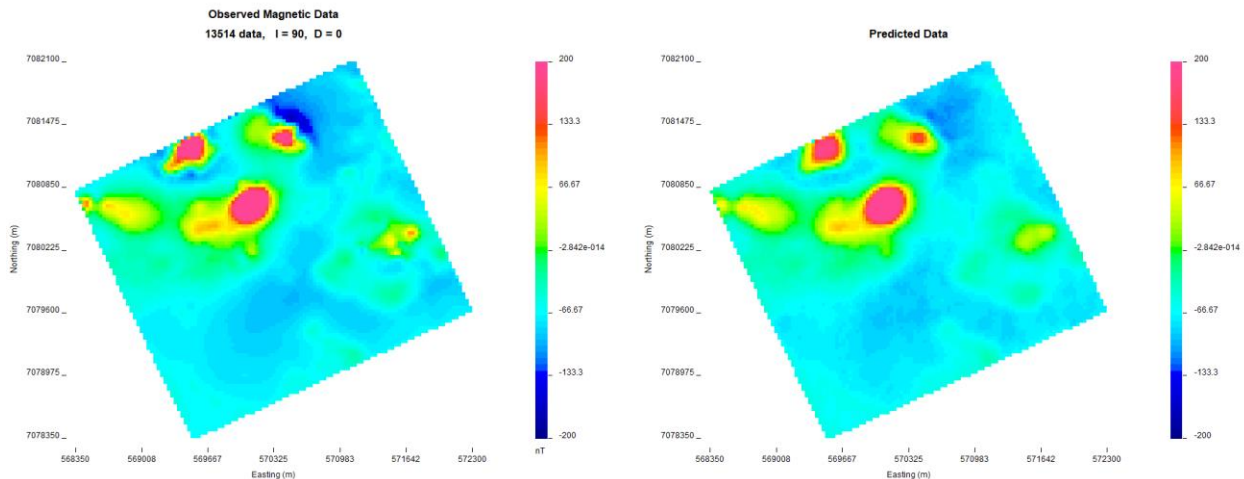


Figure 7: Observed magnetic data (Left) and predicted data from the recovered detailed susceptibility model (Right) of the IND 2017 airborne magnetic data.

Figure-8 and Figure-9 show a horizontal slice at 700m above sea level for regional and 800m above sea level for detailed magnetic susceptibility models. The detailed magnetic susceptibility model is best viewed in 3D using a variety of views with different slices, cut-off values, and colour-scales. The horizontal slices, vertical sections and iso-surfaces convey the main features of the inverted magnetic susceptibility model. All magnetic susceptibility model values are in SI unit. A 3D view of magnetic susceptibility greater than 0.005 SI and 0.01 SI for a detailed inversion block are shown in Figure-10.

For the detailed local magnetic inversions, the maximum value reaches above 0.1 SI could be sufficient for self-demagnetization effects to be considered in some regions.

Higher susceptibilities than this are probable as the model value represents the bulk volume susceptibility for the entire cell, and it is likely that it represents a combined effect of higher and lower susceptibilities at the sub-cell. In addition, the smooth-model inversion procedure often underestimates the property value. The models show detailed structure near the surface and gradually more smooth structure with depth which reflects the resolution of the magnetic method. Observed and predicted data are included in the deliverables for comparison and analysis.

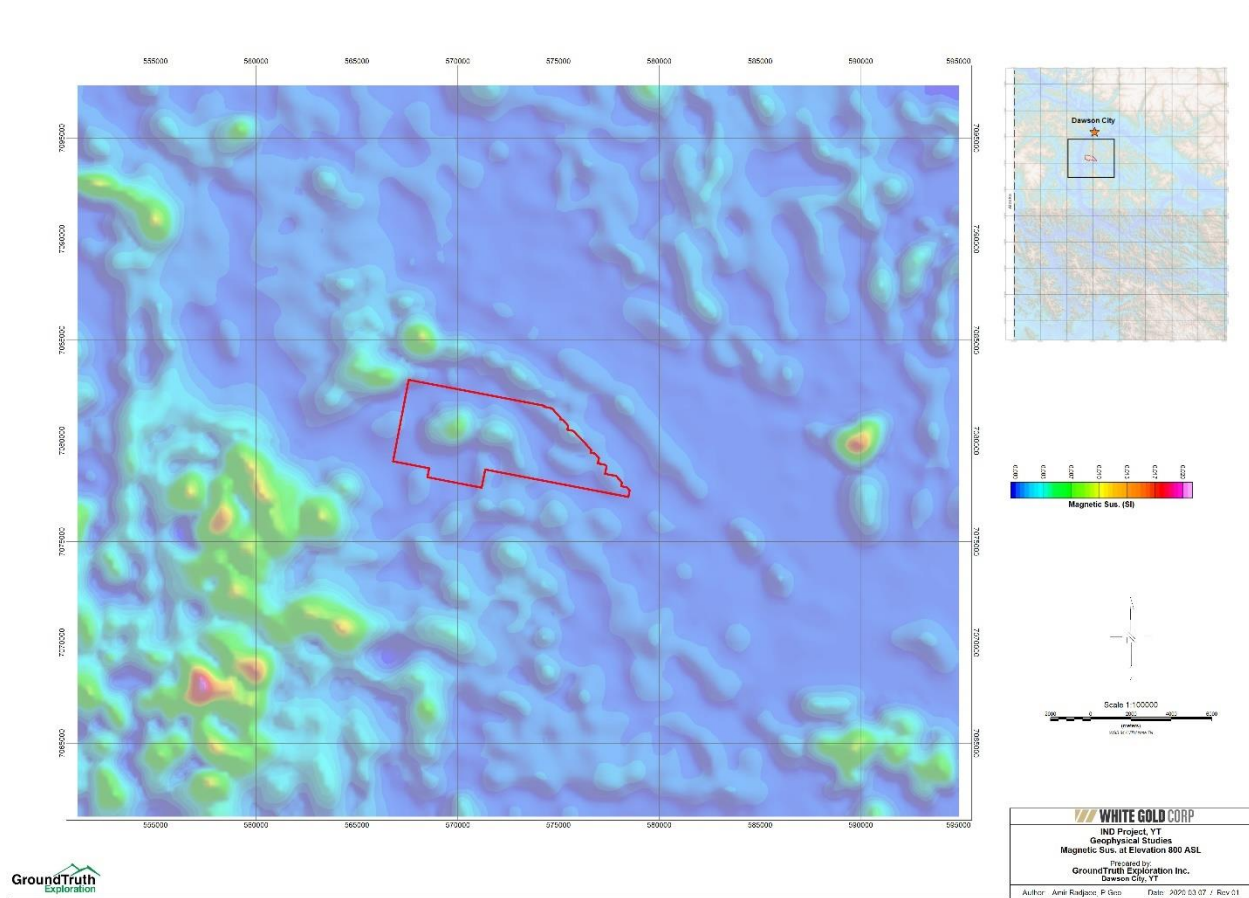


Figure 8: The horizontal slice at 800m above sea level for regional magnetic susceptibility model.

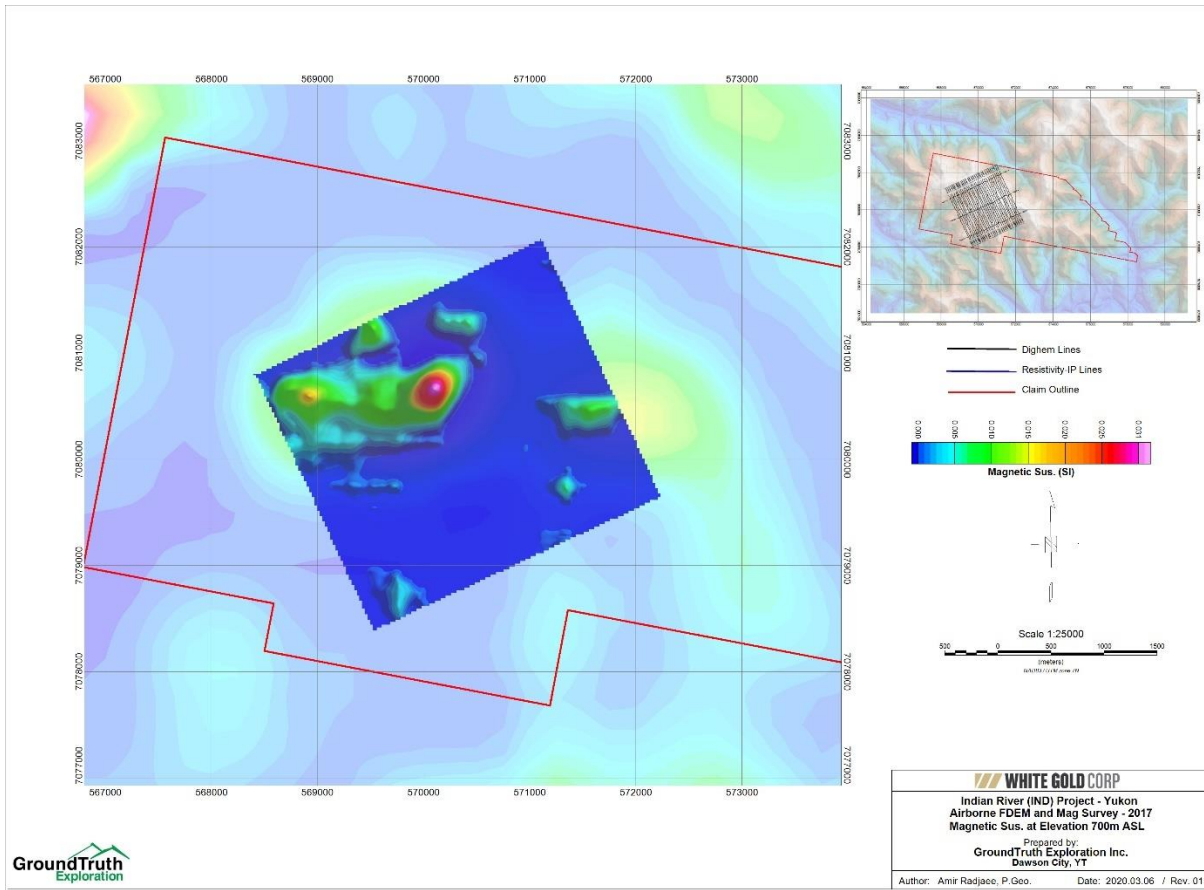


Figure 9: The horizontal slice at 700m above sea level for detailed of magnetic susceptibility model.

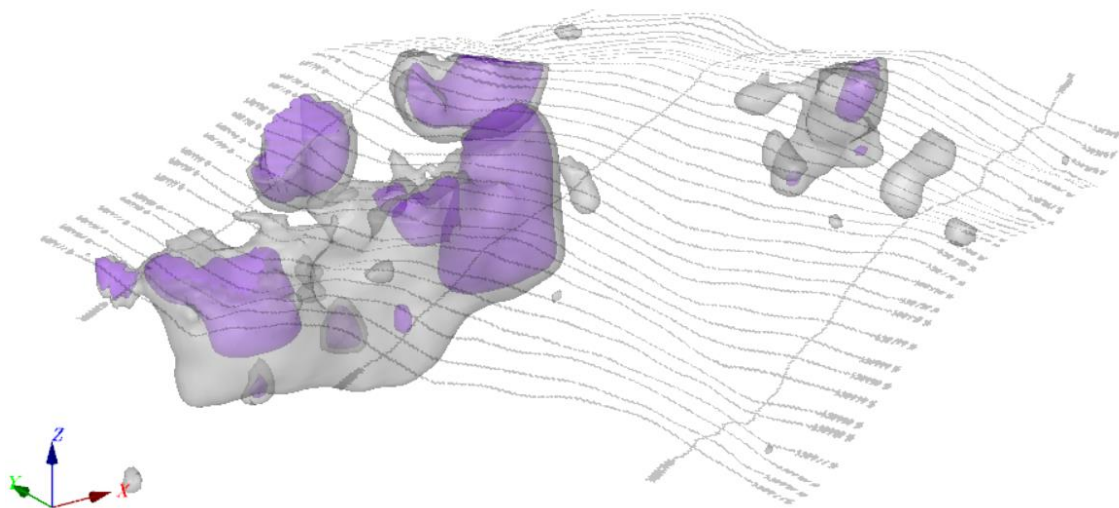


Figure 10: 3D view of high magnetic susceptibility areas greater than 0.005 SI (gray) and 0.01 (purple) SI for detailed inversion block (view NW).

Box 70, DAWSON, YT
Y0B 1G0

4.0 1D inversion modeling of EM data

The airborne frequency-domain EM (FDEM) inversions were performed using the 1D electromagnetic inversion program EM1DFM developed at the University of British Columbia – Geophysical Inversion facility (UBC-GIF). This inversion program is designed to construct any type of geophysical frequency domain loop-loop data.

The input to the inversion algorithm is the in-phase and/or quadrature components of the secondary H-field normalized by the primary field in ppm, assigned data uncertainties, distance between transmitter and receiver loops and altitude, and model and inversion parameters (e.g. layer thicknesses, background conductivity, and level of desired data misfit). The outputs are a finely discretized 1D conductivity model for each sounding, the predicted data, and a number of measures which can be used to evaluate the quality of the inversion results. The recovered conductivity is smoothly varying in depth while at the same time it is minimally different from the prescribed reference conductivity. It predicts the observed data to an appropriate degree that is justified by the assigned errors in the data.

Each sounding is inverted individually. The 1D conductivity models are presented side-by-side along line and also interpolated between lines to create approximate 3D conductivity models of the earth.

Because of the large area covered by AEM surveys, the host geology will often vary considerably. In terms of the EM survey, this means the background conductivity will change over the survey area. For the inversions being performed on these data, the reference conductivity model should be varied accordingly. Also, the level of data misfit is often hard to determine for each sounding along a line because noise levels in the data vary and also 3D conductivity features may be encountered that may not be explained with a 1D model thus choosing the level of data-misfit can be difficult.

In order to help avoid these problems, a laterally parameterized methodology is followed for the inversion of airborne EM data. First the best-fitting half-space models are calculated. These half-space values are smoothed laterally along line and then used as reference model inputs for the layered inversions. This provides a gradually changing background conductivity, results in more consistent models from sounding to sounding, and reduces misleading conductivity modelling artifacts. The smoothed background conductivity model is also a useful exploration product when displayed as a map as it shows lateral variations in conductivity that can be a guide to deeper, underlying geology. The inversions are subsequently re-run with the smoothed estimate of the trade-off parameter used at each sounding. The resulting models are more consistent from sounding to sounding and allow for geologic features to be more easily interpreted.

The in-phase and quadrature data are inverted for a 1D (layered earth) conductivity model using the UBCGIF-EM1DFM inversion code. Stations were inverted for a 1D earth distribution of conductivity using 80 layers with thickness of 2m, and with a total depth of 160m. Padding cells of increasing dimensions extending vertically down complete the layered earth used in the inversion. Padding cells are removed for deliverable model products. The 1D inversion models have been interpolated in 3D. The resistivity sections along the survey lines and depth slices were extracted later from interpolated 3D model.

The depth of investigation depends upon the EM instrumentation and survey parameters, and also upon the conductivity structure. The depth of investigation can be estimated by carrying out multiple inversions using different backgrounds (as is done in DC resistivity inversion) but it can also be estimated using cumulative conductance rules which is used here and the resulting models are cut-off below this depth and provide a guide to the depth to which more reliable interpretation can be made.

The resistivity model at depth 40m is shown in Figure-11. The 2D sections extracted from resistivity model is expected to show some correlation to the geology but will not show the bedrock where overlying conductive units are present. A 3D view of conductivity iso-surfaces with some resistivity sections along survey lines is shown in Figure-12.

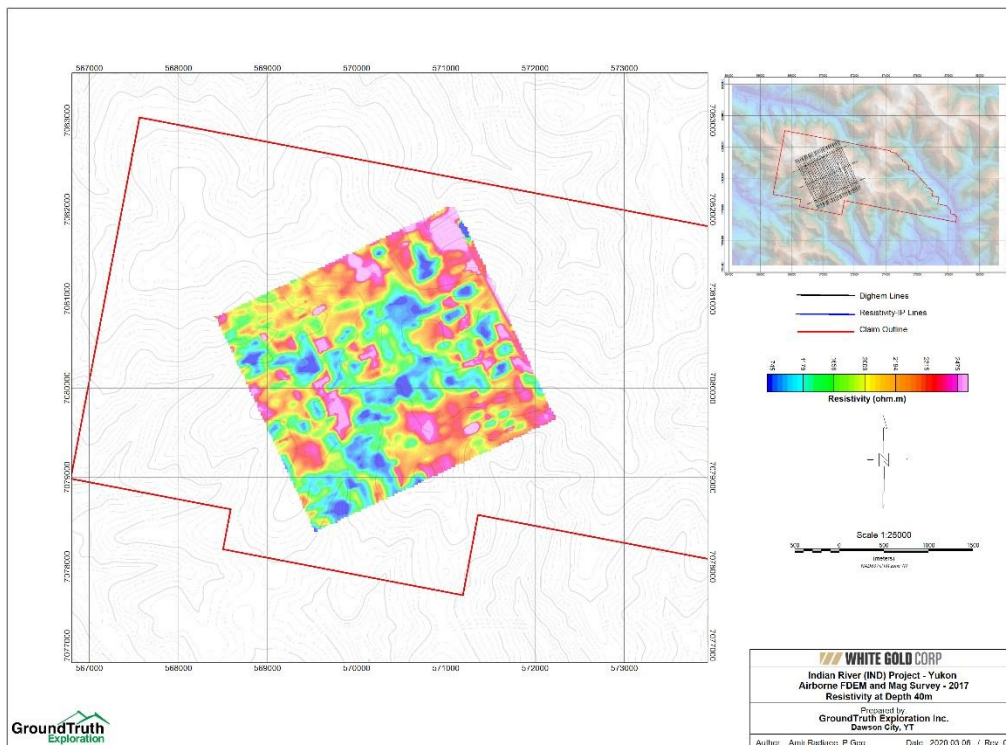


Figure 11: The resistivity depth slice at 40m below surface extracted from interpolated 3D model.

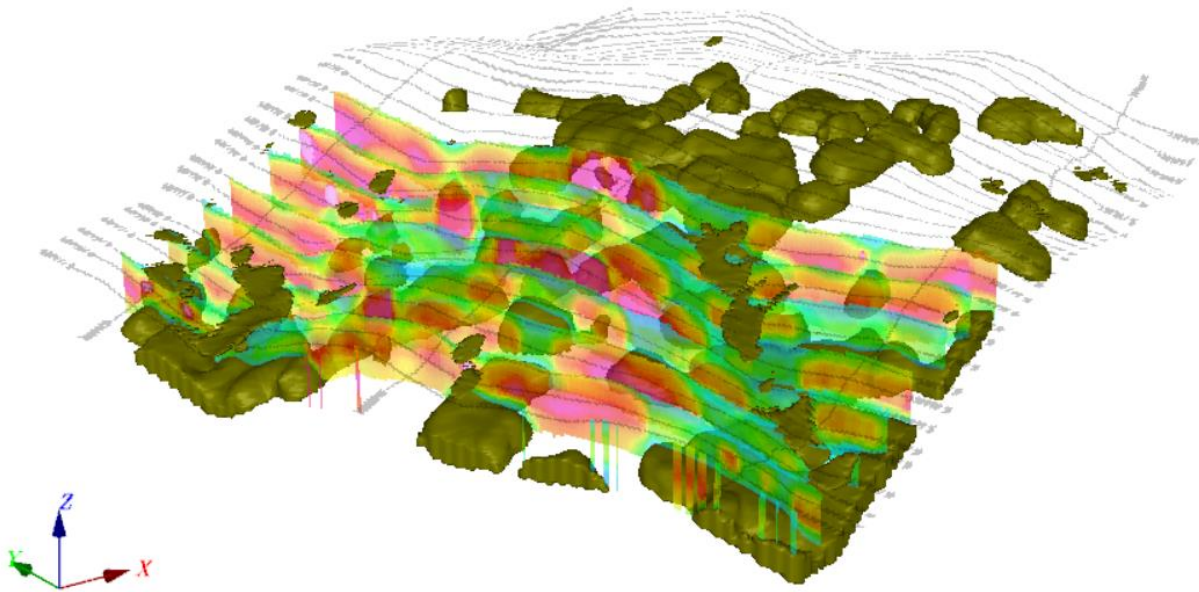


Figure 12: 3D view of conductive zones greater than 0.002 moho (resistivity 500 ohm.m) and resistivity sections along some of the survey lines.

5.0 Unconstrained 2D/3D inversion modeling of DCIP data

The purpose of the DC resistivity-IP (DCIP) survey is to identify geological structures and delineate extent of mineralized zones that are indicated by soil anomalies. The resistivity and IP inversions were performed using the 2D inversion program RES2DINV and 3D inversion program RES3DINV developed by Geotomo Software. The software is capable of producing L2 (smooth) and L1 (blocky) model results but the L2 option is most commonly used. This means that sharp boundaries will appear somewhat smoothed.

The data were acquired by GroundTruth Exploration on 2017 through a AGI Supersting resistivity meter along 15 survey lines. Each line consists of 84 electrodes with equivalently spaced along the line at 5m and hammered to a depth of 50cm. The measurements acquired in the field were processed in 2D by the RES2DINV program first resulted in sections, and then in 3D by RES3DINV resulted in 3D block models of resistivity and chargeability.

The 3D mesh was composed by 14 parallel profile lines with 100m and 200m line spacing. The inversions were run using 15 layers increasing in thickness from 2m to 12m with a total depth of about 100m. The horizontal mesh size is 20m x 20m. Padding cells of

increasing dimensions extending east, west, north, south, and vertically down complete the volume used in the inversion. The padding cells help accommodate signals that cannot easily be accounted for the core mesh. Padding cells are removed for deliverable model products.

Model resistivity and chargeability are then adjusted iteratively until the calculated data values match the observed data as closely as possible. The resistivity and chargeability models were then imported to Geosoft Oasis montaj for georeferencing from grid coordinates to UTM, and for 3D visualization.

Figure-13 and 14 show resistivity and chargeability models at depth 40m. A 3D view of low resistivity and high chargeability anomalous zones are shown in Figure-15.

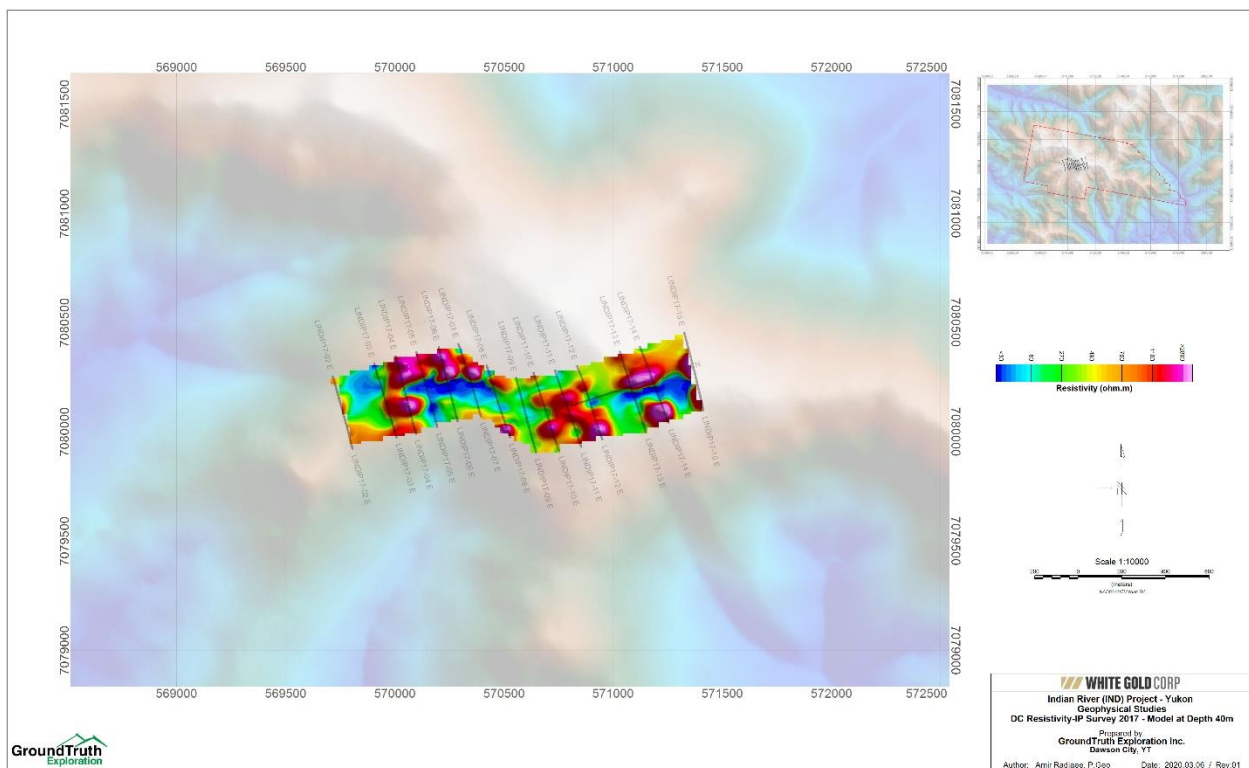


Figure 13: Resistivity depth slice at 40m below surface extracted from 3D inversion of DCIP data.

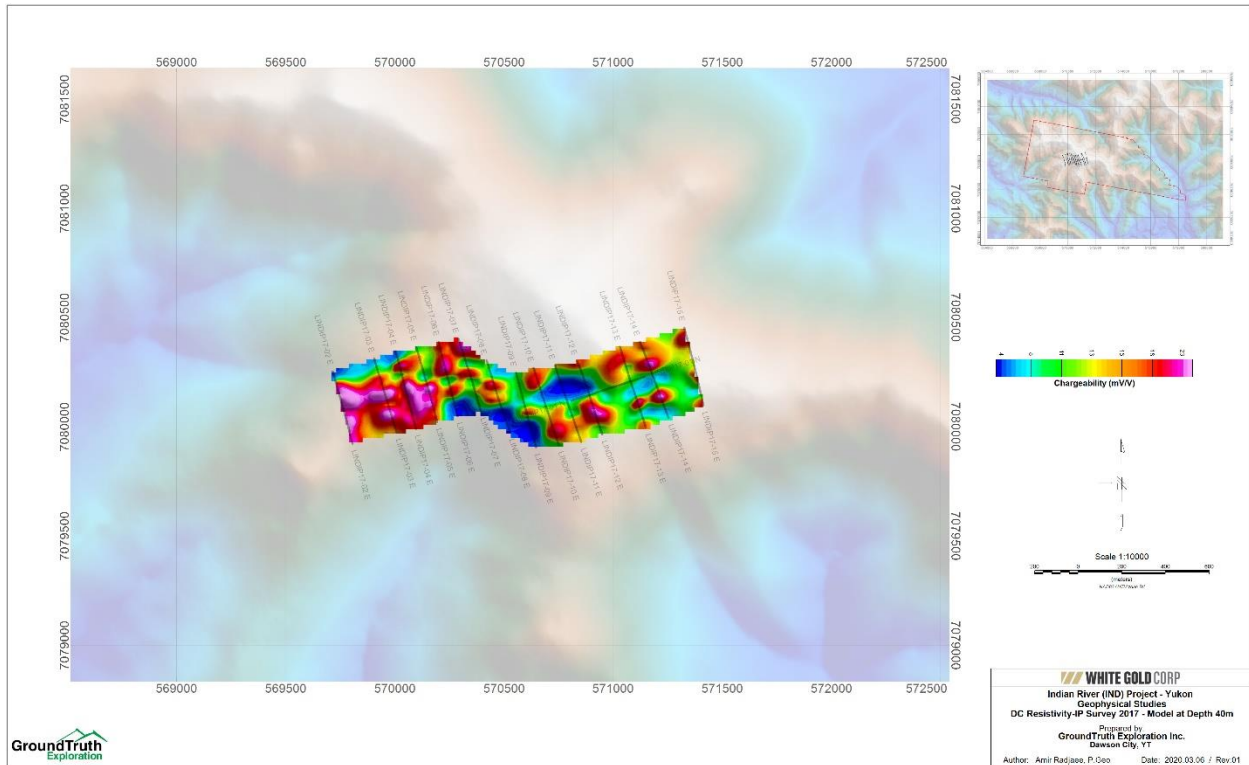


Figure 14: Chargeability depth slice at 40m below surface extracted from 3D inversion of DCIP data.

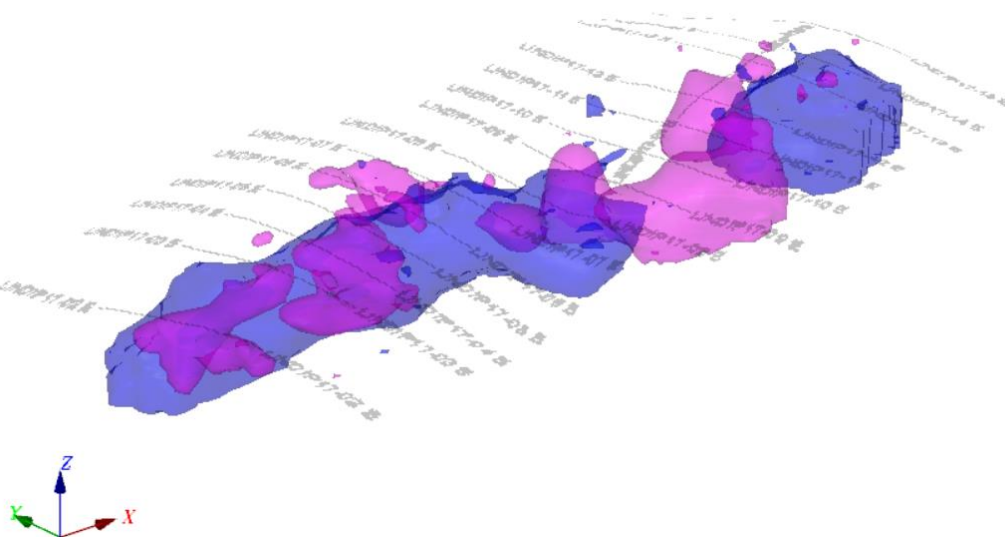


Figure 15: Low resistivity lesser than 100 ohm.m (blue) and high chargeability greater than 20 mV/V (purple) iso-surfaces from 3D inversion of DC resistivity-IP data.

6.0 Integration of data and Interpretation

The 2D and 3D magnetic susceptibility, resistivity and chargeability models can be integrated into 3D formats for detail analysis and visualization. This will ensure that 3D geological models respect a consistent structural, stratigraphic, and topological framework in addition to ensuring consistency between different geophysical models.

The geologic setting of epithermal deposits includes faulted, fractured, and brecciated rocks. Predominantly, magnetic signatures of epithermal deposits can be characterized as short-wavelength magnetic anomalies that are common over volcanic terranes because of variable magnetizations and polarizations. This pattern may contrast with an area of moderate to intense alteration that will display a longer-wavelength low, often linear in the case of vein systems, caused by the destruction of magnetite. Local magnetic highs may be associated with intrusions as well as alteration areas rich in magnetite. Magnetic lows will be associated with alteration; however, discriminating such lows from the background may be difficult on a deposit scale.

Figure-16 shows the RTP magnetic residual resulting from the 200m upward continuation of gridded data. The RTP magnetic residual and some other derivative products of this grid were used for the mapping of regional magnetic linear features/lineaments. The interpreted lineaments mapped from these grids can better identify lithological and structures features as well as the possible shear and fracture zones. The linear conductors mapped from the airborne EM 2017 survey are shown in Figure-17 and 18.

The resistivity and chargeability depth slices at 40m extracted from the 3D model of DCIP 2017 data are presented in Figure-19 and 20. Figure-21 shows magnetic susceptibility >0.01 SI, resistivity <100 ohm.m, and chargeability >20 mV/V iso-surfaces from 3D models are plotted over gold assay grid from soil geochemical data.

Most of the conductive zones are associated with low resistivity (high conductivity) areas identified by 3D inversion modelling of DCIP data. Some high chargeability anomalies overlain high gold areas mostly near the edges of low resistivity zones. The EM results define a pronounced E-W trending conductors mapped from EM in-phase and quadrature waveforms at different frequencies. These conductors are sub-parallel with the magnetic lineaments mapped from aeromagnetic data and also correlated with the general trend of the Au geochemical anomalous zone (Figure-21).

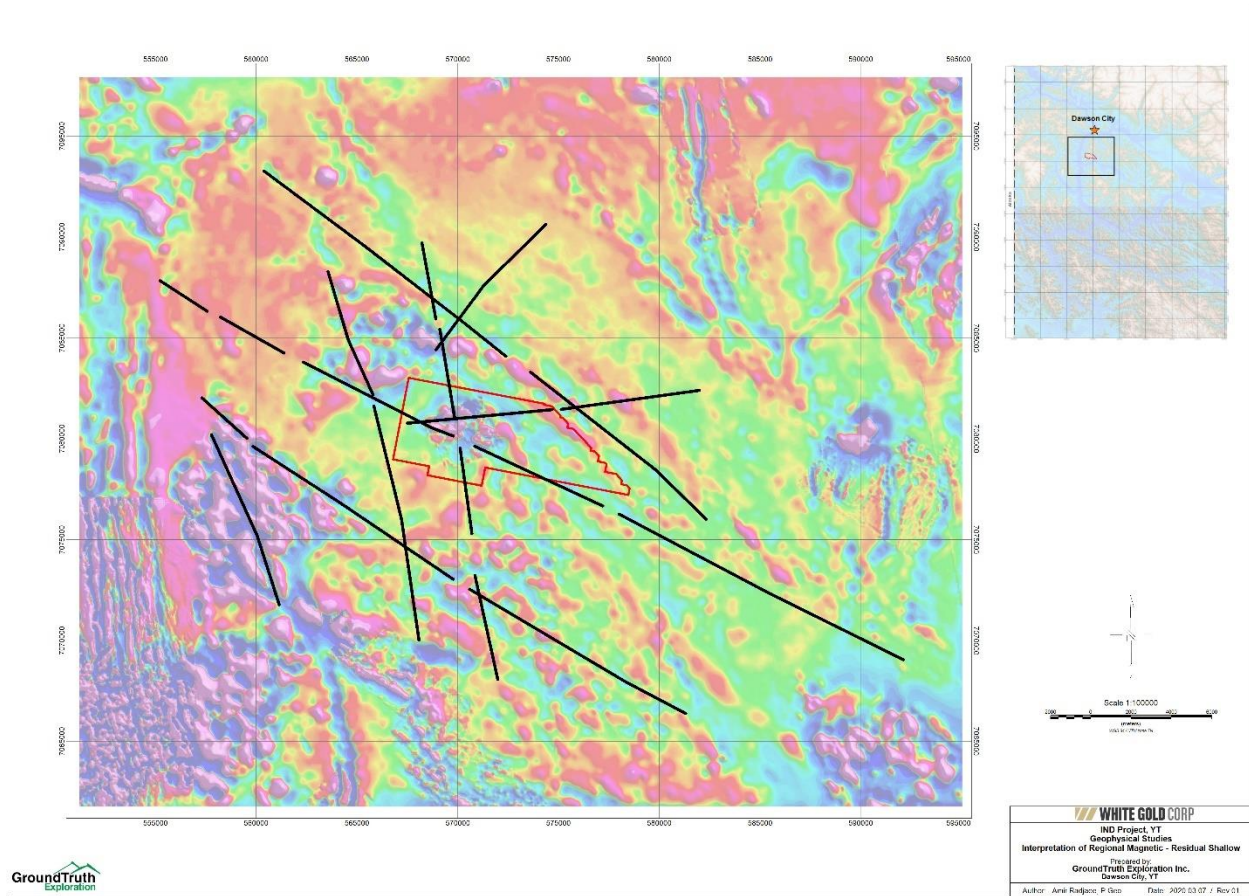


Figure 16: The RTP magnetic residual resulting from upward continuation. The interpreted lineaments can better identify lithological and structures features as well as the fracture zones are mapped from regional compiled magnetic data.

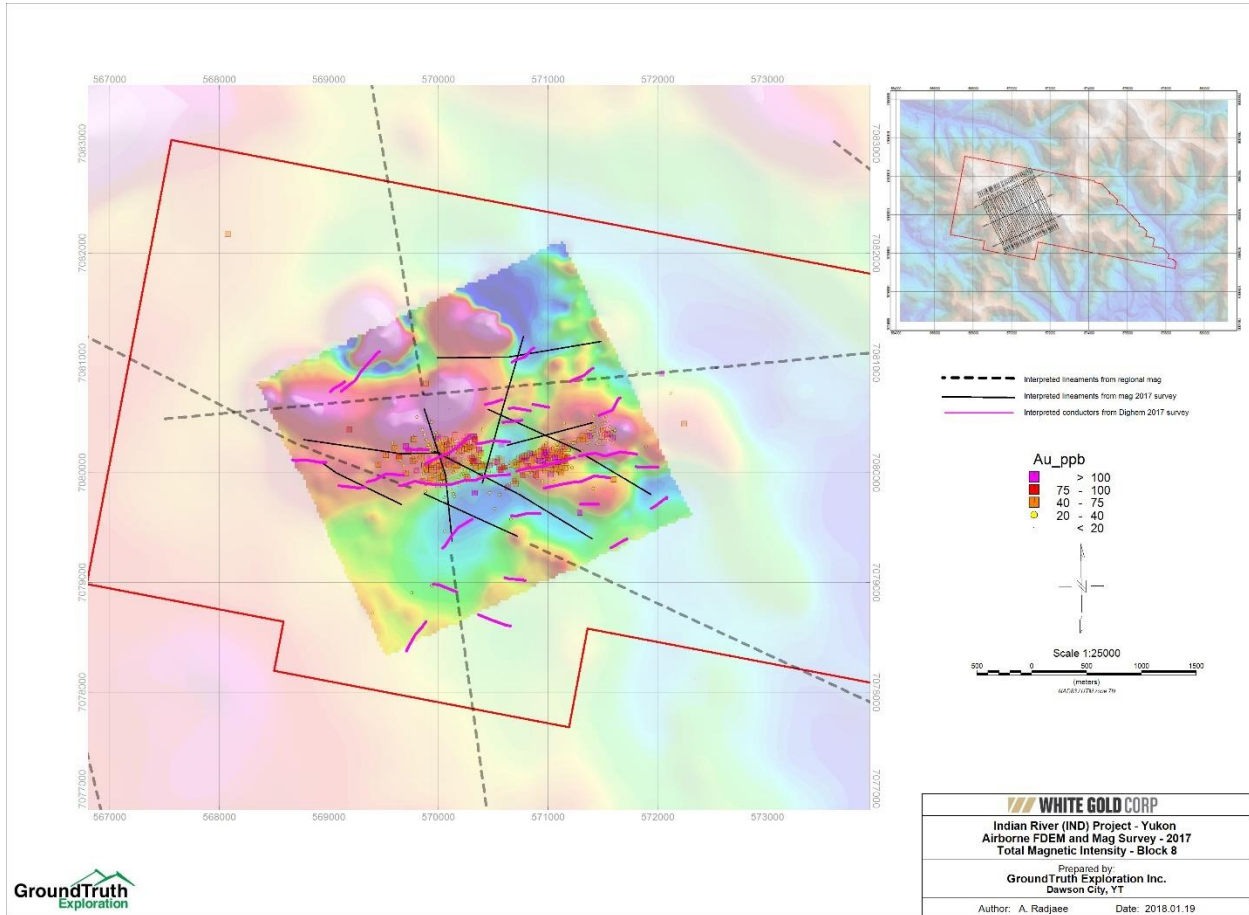


Figure 17: Background is the regional RTP magnetic, the foreground is RTP magnetic of aeromagnetic survey 2017 after regional removal. The interpreted lineaments can better identify lithological and structures features as well as the fracture zones. The dashed lines are mapped from regional compiled magnetic data, the solid black lines are mapped from 2017 magnetic survey. The purple lines are conductors mapped from airborne EM 2017 survey.

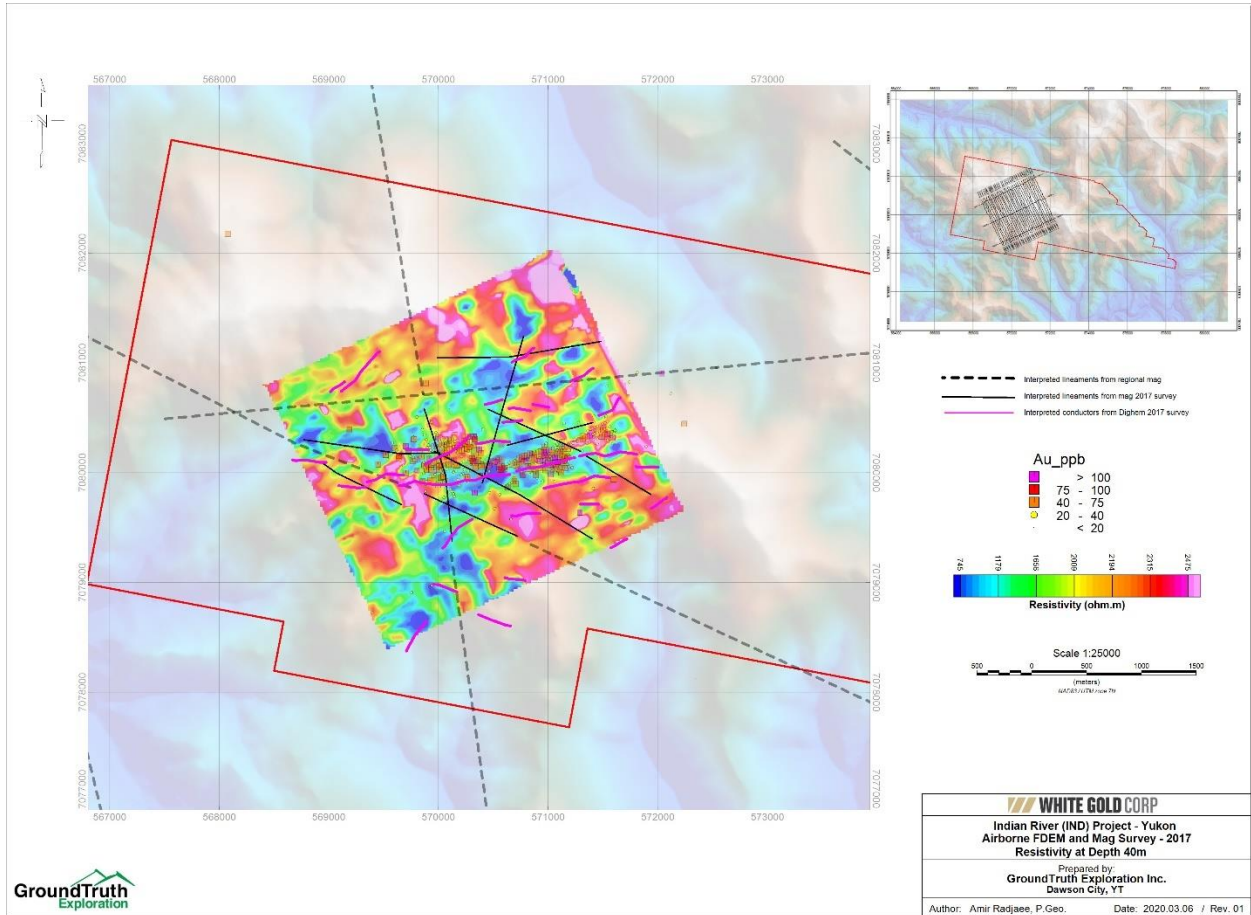


Figure 18: Resistivity depth slice from inversion modelling of Dighem 2017 survey at 40m below the surface. The dashed lines are mapped from regional compiled magnetic data, the solid black lines are mapped from 2017 magnetic survey. The purple lines are conductors mapped from airborne EM 2017 survey.

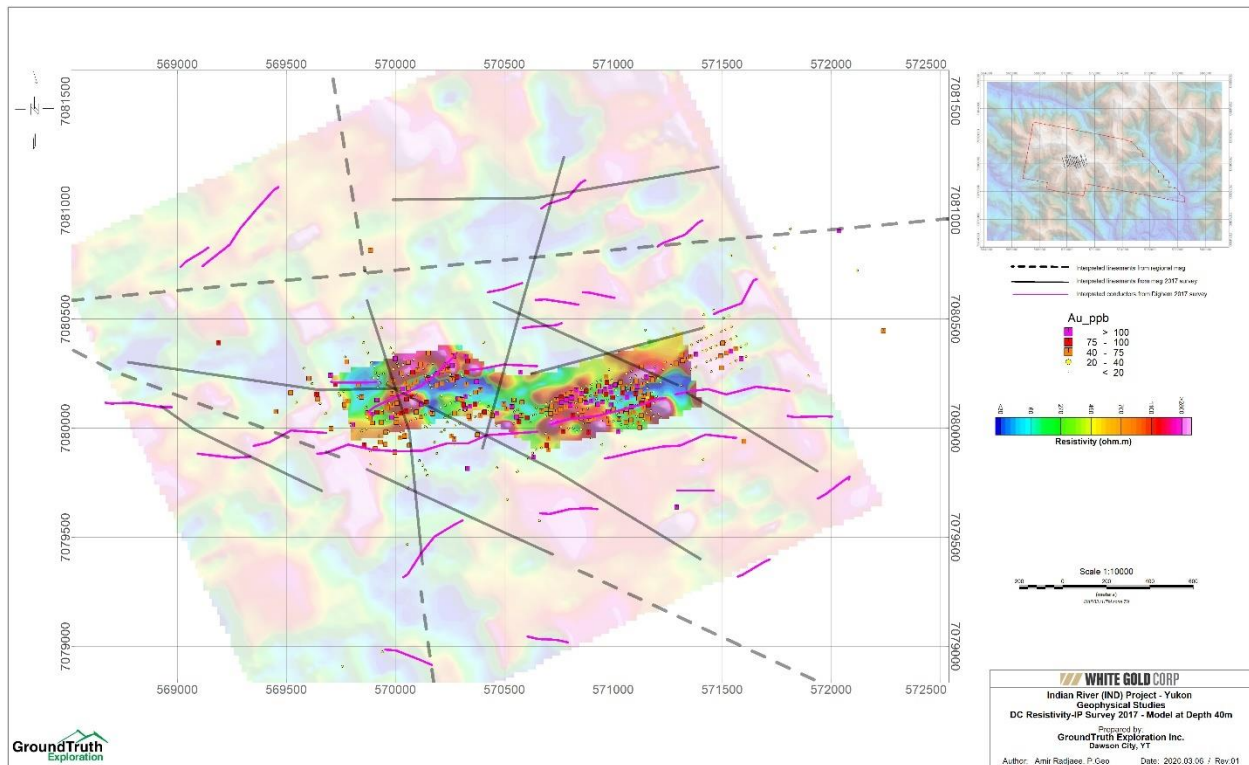


Figure 19: Background is the resistivity depth slice from inversion modelling of Dighem 2017 survey, the foreground is resistivity depth slice from DC resistivity-IP 2017 survey both at 40m below the surface. The interpreted lineaments can better identify lithological and structures features as well as the fracture zones. The dashed lines are mapped from regional compiled magnetic data, the solid black lines are mapped from 2017 magnetic survey. The purple lines are conductors mapped from airborne EM 2017 survey.

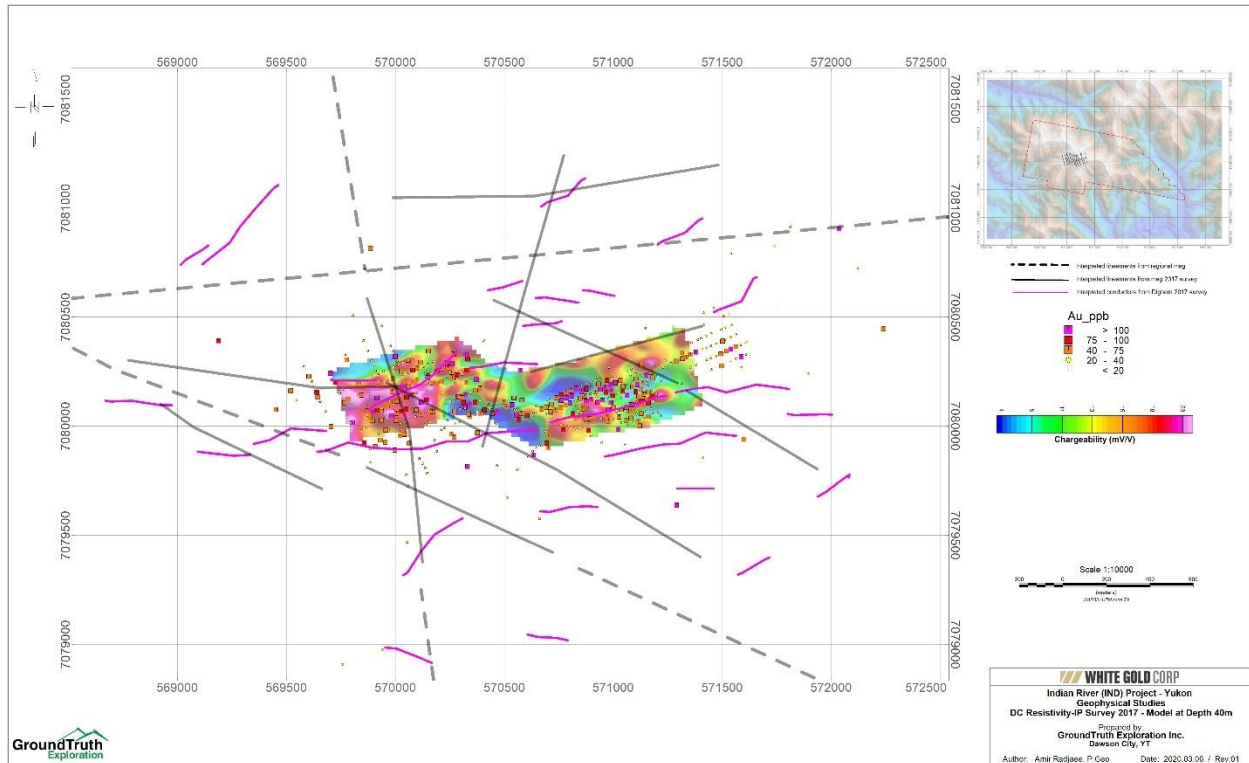


Figure 20: The chargeability depth slice from DC resistivity-IP 2017 survey at 40m below the surface. The interpreted lineaments can better identify lithological and structures features as well as the fracture zones. The dashed lines are mapped from regional compiled magnetic data, the solid black lines are mapped from 2017 magnetic survey. The purple lines are conductors mapped from airborne EM 2017 survey.

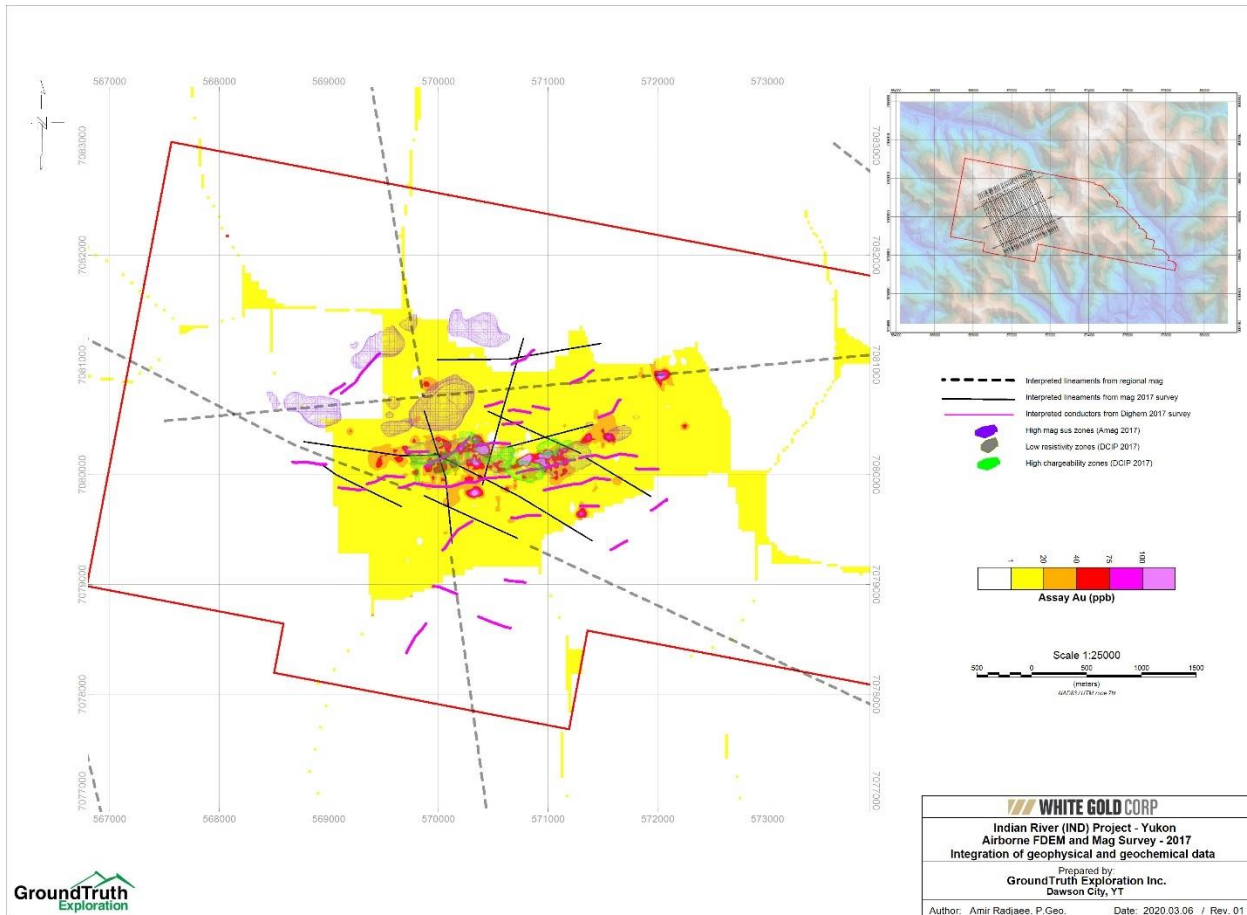


Figure 21: Background is gold assay from soil geochemical data. The magnetic susceptibility, resistivity and chargeability iso-surfaces from inversion modeling are plotted in purple, gray and green. The interpreted lineaments can better identify lithological and structures features as well as the fracture zones. The dashed lines are mapped from regional compiled magnetic data, the solid black lines are mapped from 2017 magnetic survey. The purple lines are conductors mapped from airborne EM 2017 survey.

7.0 Conclusions and Recommendations

Regional and detailed, magnetic susceptibility, conductivity, resistivity, and chargeability models have been produced by different inversion modelling efforts for the IND property, YT, Canada. These models and the deliverables enclosed to this report will aid the visualization and interpretation of the data to target future exploration on the IND property. As well as the modelling products, the work undertaken in modelling preparation is valuable quality control of the data.

The deeper magnetic susceptibility models can be interpreted within the context of geology in order to help define large structures and intrusives. The laterally parameterized conductivity model will be useful in determining 3D distribution of the

conductive bodies and the depth of investigation estimate will guide reliability of the interpretations. The background conductivity model may be useful in characterizing larger scale lateral variations of the near-surface, and the linear conductors mapped from EM different waveforms will be useful for demonstrating the structural features.

Although a magnetic susceptibility, conductivity, resistivity and chargeability models has been delivered, it is recognized that other models could have been chosen as appropriate model candidates. Inverse problems are non-unique, and the output depends upon many factors that are difficult to quantify. The three main factors common to all inversions are:

- How to estimate uncertainties in the data
- Details of the model objective function and the priori information
- Determining the appropriate value of the regularization parameter that balances misfit and the model objective function

Considerable care has been taken to remove regional fields prior to the merging process of magnetic data, estimating errors for all inversions, incorporating reasonable information into inversion modelling, and generating inversion models of different physical properties that fit the data well but do not over-fit the data. In addition, because the inversion algorithms attempt to find the simplest or generally smooth models that fit the data, the provided models will hopefully be representative of the larger-scale features in the earth.

In a 3D GIS frame, the distribution of physical properties can help to identify potential exploration areas, and in follow-up work in these local regions, inclusion of additional information in the form of geologic knowledge (conceptual model, overburden thickness, drilling, outcrop lithology, etc.), petrophysical information, and further geophysics, will help guide the selection of inversion parameters and constraints so that models with enhanced resolution can be obtained. This should make exploration more successful and cost-effective.

For 3D physical property models to be used effectively for interpretation and exploration targeting, a good understanding of the exploration target physical properties will be needed which can be related to geology and geologic processes. Integrated interpretation and 3D GIS analysis on the magnetic susceptibility model can be customized to specific exploration target criteria. In order to continue the construction of a 3D Earth model with multiple earth properties useful for exploration targeting, more layers of information such as different geophysical data or models, geochemical data, drilling, and geologic mapping and structural information can be added.

If geologic or physical property information is made available, the models can be recreated with this information acting as a constraint on the inversion process. This would produce more reliable models that are consistent with multiple data sets.

The magnetic inversion modelling did not account for either remanent or self-demagnetization affects. In some areas, these may be present, and it will be important to understand the effect more complicated magnetization has on the data in order to avoid misleading interpretations.

Data acquired as the follow-up to targeting from the physical property models or other data (e.g. geochemical data) can be collected using effective survey designs based on physical property analysis and the inversion models. This will ensure appropriate sensitivity to the exploration target is obtained. Due to the remarkable correlation of geochemical anomalies with low resistivity zone, the ground VLF/Mag with a maximum line spacing of 50m is recommended for further follow-up. The VLF data can be processed by the 2D inversion program VLF2Dmf and provide the exploration team with a more detailed resistivity model. Also, DC Resistivity and IP survey can be designed to target a magnetic susceptibility body at an estimated depth with a known geochemical anomalous zone. This knowledge will allow feasibility studies to optimize the survey parameters, so the goal of the survey is efficiently realized.

8.0 Submittal

The work in this report has been completed by Amir Radjaee Senior Geophysicist of the GroundTruth Exploration under supervision by Isaac Fage Operational Director of the GroundTruth Exploration.

9.0 Deliverables

Report in pdf format

- Compilation, processing and interpretation of geophysical data for IND
March 14, 2020

Autocad DXF format

- Iso-surfaces for mag susceptibility, resistivity and chargeability

Grids in Geosoft format

- RTP grids and derivative products for regional and property scale data
- Depth and elevation horizontal slices for mag susceptibility, resistivity from AEM, resistivity and chargeability from DCIP

- Georeferenced grid sections for resistivity from AEM

ArcView Shapefiles

- Survey lines for airborne and DCIP 2017 surveys
- Mag lineaments interpreted from regional and property scale mag data
- Conductors interpreted from AEM

Maps in pdf format

- All maps used for figures in this report

Magnetic sus 3D model in UBC format

- UBC model and mesh files for mag susceptibility, resistivity and chargeability

10.0 References

Donegal Developments Ltd., Assessment Report, 2007, HELICOPTER MAGNETIC AND RADIOMETRIC SURVEY FOR LOGAN RESOURCES LTD.

EM1DFM Manual 2000, UBC-GIF, Earth and Ocean Sciences,

<https://em1dfm.readthedocs.io/en/latest/>

H. Smith, Assessment Report, 2009, VTEM AND MAGNETIC SURVEY at the IND MOUNTAIN PROPERTY.

Li, Y. and Oldenburg, D.W., 1996, 3-D inversion of magnetic data, Geophysics, 61, 394-408.

Li, Y. and Oldenburg, D. W., 1998b, Separation of regional and residual magnetic field data, Geophysics, 63, 431-439.

M.W.P. Hibbitts and T.E.P. Nillos, 2006, GEOLOGICAL AND GEOPHYSICAL REPORT ON THE CHEYENNE PROPERTY, DAWSON MINING DISTRICT, YT, CANADA.

MAG3D, A Program Library for Forward Modelling and Inversion of Magnetic Data over 3D Structures, Version 5.0 <https://gif.eos.ubc.ca/sites/default/files/mag3dManual.pdf>

Mira Geoscience Ltd., 2011, Regional 3D inversion modelling of airborne gravity, magnetic, and electromagnetic data, Central BC, Canada, Geoscience BC, Geoscience BC Report Number: 2011-15.

Oldenburg D.W., Li Y., Farquharson C.G., Kowalczyk P., Aravanis T., King A., Zhang P., and Watts A, 1998, Applications of Geophysical Inversions in Mineral Exploration Problems, The Leading Edge, 17, 461 - 465.

Total Energold Corporation, 1989, Geological and Geochemical Report on the Buz 1 - 14, and HUD 1-6 and Tooth 1-1 80 Claims. Assessment # 092787.

11.0 Statement of Qualifications

I, Amir H. Radjaee, of the city of Vancouver, Province of British Columbia, do hereby certify that:

- 1- I am a Senior Geophysicist at GroundTruth Exploration Inc. Ltd with business address: 109 Callison Way, Dawson City, YT, Y0B 1G0, Canada.
- 2- I graduated with a Master of Science (MSc) degree in Geophysics from the University of Tehran and Doctor of Philosophy (PhD) degree in Geophysics from the International Institute of Earthquake Engineering and Seismology.
- 3- I have been employed in my profession as a Geophysicist for over 15 years since my graduation.
- 4- I am a member of Association of professional Engineers and Geoscientist of the Province of British Columbia, License# 36294.
- 5- The information for this report is based on available data explained in the Introduction section of this report and from the results derived from further modelling and post-processing works.
- 6- I have no interest in the property described as the White Gold Corp, nor do I have any plans to acquire any such interests.

Dated this 14th day of March, 2020, Vancouver, B.C



3D INVERSION MODELING AND INTERPRETATION OF
AIRBORNE MAGNETIC DATA

Appendix-A

Modelling Software
UBC-GIF MAG3D and EM1DFM

MAG3D is a program library (version 5.0 as of September 2013) for carrying out forward modelling and inversion of surface, airborne, and/or borehole magnetic data in the presence of a three dimensional Earth. The program library carries out the following functions:

- Forward modelling of the magnetic field anomaly response to a 3D volume of susceptibility contrast.
- Data are assumed to be the anomalous magnetic response to buried susceptible material, not including Earth's ambient field.
- The model is specified using a mesh of rectangular cells, each with a constant value of susceptibility, and topography is included.
- The magnetic response can be calculated anywhere within the model volume, including above the topography, simulating ground or airborne surveys, and inside the ground simulating borehole surveys.

This inversion code assumes susceptibilities are "small". This means results will be wrong when susceptibilities are high enough to cause self-demagnetization. There is no method for incorporating remanent magnetization in this code.

Inversion of surface, airborne, and/or borehole magnetic data to generate 3D models of susceptibility contrast. The inversion is solved as an optimization problem with the simultaneous goals of minimizing an objective function on the model, and generating synthetic data that match observations to within a degree of misfit consistent with the statistics of those data. To counteract the inherent lack of information about the distance between source and measurement, the formulation incorporates a depth or distance weighting term. By minimizing the model objective function, distributions of subsurface susceptibility contrast are found that are both close to a reference model and smooth in three dimensions. The degree to which either of these two goals dominates is controlled by the user by incorporating a priori geophysical or geological information into the inversion.

Explicit prior information may also take the form of upper and lower bounds on the susceptibility contrast in any cell (as of version 5.0). The regularization parameter (controlling relative importance of objective function and misfit terms) is determined in either of three ways, depending upon how much is known about errors in the measured data.

The large size of useful 3D inversion problems is mitigated by the use of wavelet compression. Parameters controlling the implementation of this compression are available for advanced users (MAG3D Manual).

Program EM1DFM is designed to construct one of four types of 1D models, using any type of geophysical frequency domain loop-loop data using one of four variations of the inversion algorithm.

The observations are the inphase and/or quadrature components of the secondary H-field normalized by the primary (i.e., free-space) field in ppm, or the secondary H-field normalized by the primary field in %, or the secondary H-field in A/m, or the total H-field in A/m.

Receiver coils can be oriented in x-, y- or z-directions, and they can be at any position relative to their respective magnetic dipole transmitter. Transmitters can be at any height, can be oriented in the x-, y- or z- directions, and any frequency or set of frequencies may be involved. All the observations (in any combination) to be used to construct the one-dimensional model at a particular horizontal location are grouped together as one "sounding". Measurement uncertainties can be in the same units as the observations or as relative uncertainties in percent.

The inversion program can construct an electrical conductivity model (with magnetic susceptibility fixed), or a strictly-positive magnetic susceptibility model (with conductivity fixed), or both conductivity and strictly-positive susceptibility models, or both conductivity and susceptibility (with no positivity constraint) models.

Models of the Earth are composed of many layers of uniform conductivity/susceptibility with fixed interface depths. The value of the conductivity/susceptibility in each layer is sought by the inversion. Multiple soundings can be handled in a single run of the program. Each sounding is interpreted independently with a one-dimensional model produced under the sounding location. When all soundings have been inverted, a composite two-dimensional model is written out to facilitate interpretation of a line of soundings.

There are four variations of the inversion algorithm constant (user-supplied) trade-off parameter in the objective function being minimized, or the trade-off parameter is automatically chosen to achieve a user-supplied target misfit, or the trade-off parameter is automatically chosen using the generalized cross validation (GCV) criterion, or the trade-off parameter is automatically chosen using the L-curve criterion.

<https://em1dfm.readthedocs.io/en/latest/>